CANADIAN THESES

THÈSES CANADIENNES

NOTICE

The quality of this microfiche is heavily dependent upon the quality of the original thesis submitted for microfilming. Every effort has been made to ensure the highest quality of reproduction possible.

If pages are missing, contact the university which granted the degree.

Some pages may have indistinct print especially if the original pages were typed with a poor typewriter ribbon or if the university sent us an inferior photocopy.

Previously copyrighted materials (journal articles, published tests, etc.) are not filmed.

Reproduction in full or in part of this film is governed by the Canadian Copyright Act, R.S.C. 1970, c. C-30. Please read the authorization forms which accompany this thesis.

AVIS

La qualité de cette microfiche dépend grandement de la qualité de la thèse soumise au microfilmage. Nous avons tout fait pour assurer une qualité supérieure de reproduction.

S'il manque des pages, veuillez communiquer avec l'université qui a conféré le grade.

La qualité d'impression de certaines pages peut laisser à désirer, surtout si les pages originales ont été dactylographiées à l'aide d'un ruban usé ou si l'université nous a fait parvenir une photocopie de qualité inférieure.

Les documents qui font déjà l'objet d'un droit d'auteur (articles de revue, examens publiés, etc.) ne sont pas microfilmés.

La reproduction, même partielle, de ce microfilm est soumise à la Loi canadienne sur le droit d'auteur, SRC 1970, c. C-30. Veuillez prendre connaissance des formules d'autorisation qui accompagnent cette thèse.

THIS DISSERTATION HAS BEEN MICROFILMED EXACTLY AS RECEIVED

LA THÈSE A ÉTÉ MICROFILMÉE TELLE QUE NOUS L'AVONS REÇUE

Canadä

Strain Based Finite Elements

For Tall Building Analysis

Martin M. Desbois

A Thesis

in

The Centre

for

Building Studies

Presented in Partial Fulfillment of the Requirements for
the Degree of Master of Engineering at

Concordia University
Montréal, Québec, Canada

September 1984

ABSTRACT

Strain Based Finite Elements
For Tall Building Analysis

Martin M. Desbois

Tall slender structures subjected to lateral loading tend to deflect in a bending mode, similarly to a laterally loaded cantilever beam. Of the numerous analysis methods, a finite analysis of such structures (shear walls, corewalls, framed tubes,...) offers a simple alternative. However, linear plane stress finite elements can be affected by .parasitic shear rendering the modelling too stiff.

Two new strain based finite elements, specifically for tall building analysis are developed. Testing shows that these elements perform well in both shear and bending deformation modes. Their fast convergence rates also enable them to be used as efficient macroelements. In the analysis of core assemblies or shear walls where the bending deformation mode is predominant, the strain based elements prove to be very efficient elements.

The macroelement technique is the method of analysis adopted in the study. The excellent performance of the

strain based elements result in the recommendation of their adoption for general use in the technique.

Deficiencies of the macroelement technique of analysis which surfaced throughout the study are pointed out and suggestions for improvement are made.

ACKNOWLEDGEMENTS

And finally, one more word, "ab uno disce omnes ..." or
"from this one specimen, learn all the rest ..."

TABLE OF CONTENTS

LIST OF FIGURES

LIST OF TABLES

NOTATIONS

a, b	Element dimensions.
A_i, i=1,10	Generalized coordinates in assumed displacement fields.
A_b, A_c, A_m	Cross-sectional area of beam, column and membrane, respectively.
A_r, A_{rb}, A_{rc}, A_{rj}	Effective shear area of lintel beam, beam, column and joint, respectively.
AR	Aspect ratio.
A_m, A_n, C_y, C_{xy}, m,	Coefficients used for evaluating the elastic properties of the equivalent membrane.
B	Bay width.
[B]	Strain-displacement matrix.
C, D	Constants.
C_1, C_2	Functions of X and Y used for determining the displacement fields.
d, d_b, d_c	depth of lintel beam, beam and column, respectively.
Dmax	Maximum lateral deflection.
DOF	Degrees of freedom.
E, G	Elastic constants of the material.
$\overline{E}_y$, $\overline{G}_{xy}$	Elastic properties of the equivalent orthotropic membrane.
[E]	Matrix of elastic constants.
H	Storey height.
I, I_b, I_c	Moment of inertia of lintel beam, beam and column, respectively.
[K]	Element stiffness matrix.
K_i, i=1,9	Stiffness coefficients in [K].
L	Span of lintel beam (or beam).

M	Applied moment.
M_b, M_c	Beam and column internal bending moments.
P	Column or membrane axial force.
Q	Lateral load.
r	Element aspect ratio $= a/b$.
t	thickness of lintel beam or membrane.
t_b, t_c, t_m	thickness of beam, column and membrane, respectively.
U, V	Assumed element displacement functions.
U_i, V_j	Element degrees of freedom.
V_b, V_c	Internal shear force in beam and column, respectively.
V_s	Shear force.
W	Applied distributed loading.
W_i, $i = 1, 4$	First four natural frequencies.
X, Y	Cartesian coordinates.
$\overline{X}$, $\overline{Y}$	Non-dimensional coordinates $= X/a$, Y/b, respectively.
Δ	Sway displacement.
ϵ_x, ϵ_y, δ_{xy}	Strain components in the equivalent orthotropic membrane.
ν	Poisson's ratio.
σ_x, σ_y, δ_{xy}	Stress components in the equivalent orthotropic membrane.
σ_{cy}, σ_{my}	Axial stress in a column and membrane (along a column line), respectively.
τ_b, τ_m	Shearing stress in a beam and membrane (along a beam line), respectively.

CHAPTER I

INTRODUCTION

1.1- GENERAL

The design of lateral load resisting systems for tall buildings is a main concern and a challenge to the structural engineer. The required lateral stiffness is generally provided by either shear walls or frames or by a combination of the two.

An efficient framing system, providing the necessary lateral stiffness for tall buildings, was introduced by Khan [16] in 1963 with the 43 storey Dewitt Chestnut Apartment Building making use of the tubular action of the interconnected facades.

Many of the world's tallest structures utilize the tube concept. Examples are: the 52 storey One Shell Plaza Building (Fig. 1.1), the 100 storey John Hancock Center (braced tube), the 110 storey Sears Tower (bundled tube) and the 110 storey World Trade Center Towers (tube in tube).

Strength, rigidity and stability are the main concerns in structural design. Strength, a dominant design factor in low-rise buildings, becomes only secondary in tall building design. As a building's aspect ratio, defined here as the ratio of total height over building depth, increases, drift control must be taken into account. Additional stiffness is
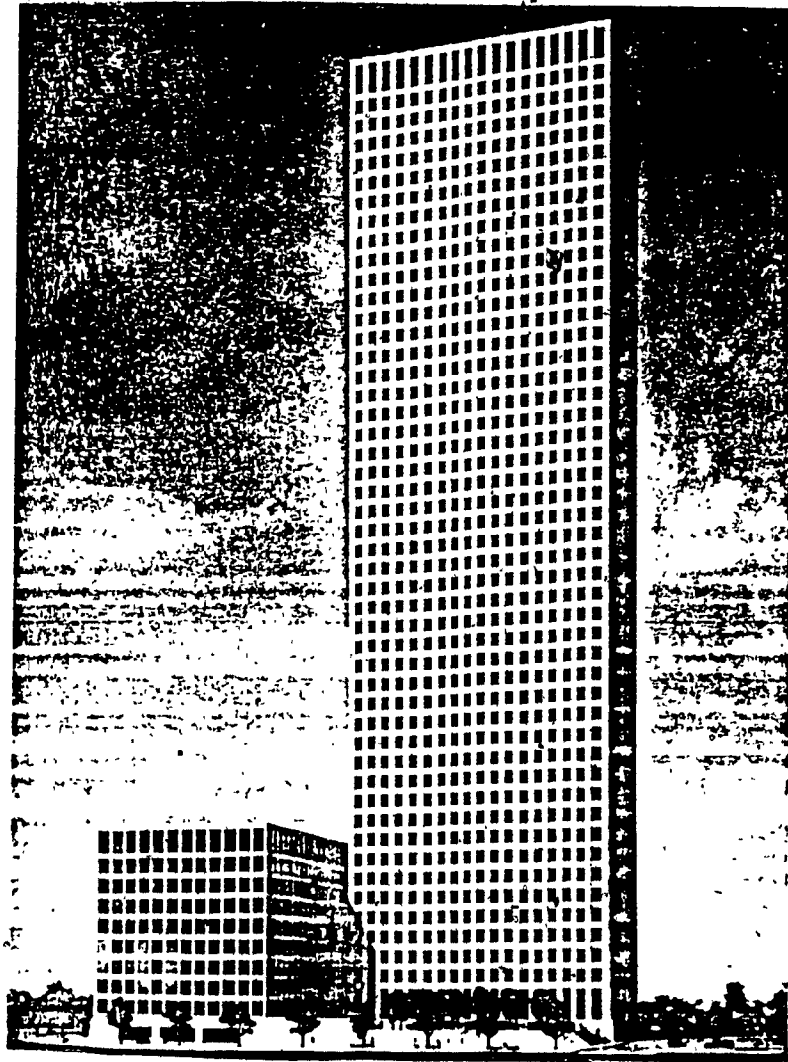
FIG. 1.1 - ONE SHELL SQUARE BUILDING (MODEL), [9]

required to maintain the lateral deflection within tolerable limits when the aspect ratio exceeds 4 or 5 [9].

Control of sway is primarily of interest to avoid discomfort to the occupants, architectural damage and detrimental effects caused by non-linear P-Δ effects [19].

The traditional beam-column framing system used in buildings of up to 30 stories becomes expensive and inadequate for providing the necessary lateral stiffness for buildings in the taller range. Members designed beyond strength requirements become fairly large and impractical. The additional lateral stiffness required for drift control must be sought elsewhere. Use of shearwalls/corewalls for lateral stiffness will normally suffice for 30-35 storey buildings [16,19]. For taller structures, the limited plan dimensions often enable the shearwalls/corewalls in acquiring the necessary depth to develop the required lateral stiffness.

A solution is brought about by distributing the material required for strength along the perimeter of the building. By using all of the available depth, one improves the efficiency of the structural system. Such systems are called tube-like structures.

The facades of tube-like structures usually come in the form of frames, braced frames or shearwalls. When the facades are composed of a beam-column framework, the structural system is called a framed tube. Ultimately, corewalls are incorporated with the framed tube system to

provide even greater stiffness. Such a system is termed tube in tube.

Tubular systems have proven to be very efficient for tall structures of both reinforced concrete and steel construction [5,8]. The framed tube system has also been shown to be economically feasible for medium-rise buildings with as few as 20 stories [16,21].

1.2- DESCRIPTION OF FRAMED TUBE SYSTEMS

The framed tube system is generally composed of three or more framed facades joined at their edges thus forming a vertical tube-like structure. The facades consist of closely spaced columns rigidily connected to short and deep spandrel beams at each floor level (Fig. 1.2).

The closely spaced columns and deep spandrel beams assure minimal flexural deformation in the members. In the framed tube system, the facades normal to the direction of applied lateral forces contribute greatly to the overall overturning strength and stiffness of the structure. Therefore, the entire structure is mobilized in resisting the applied lateral forces.

The columns are spaced anywhere from 1.22 to 4.57 m (4 to 15 feet), a common spacing being approximatively 3.0 m (10 feet). Column widths and spandrel beam depths range from .61 to 1.52 m (2 to 5 feet) [16].
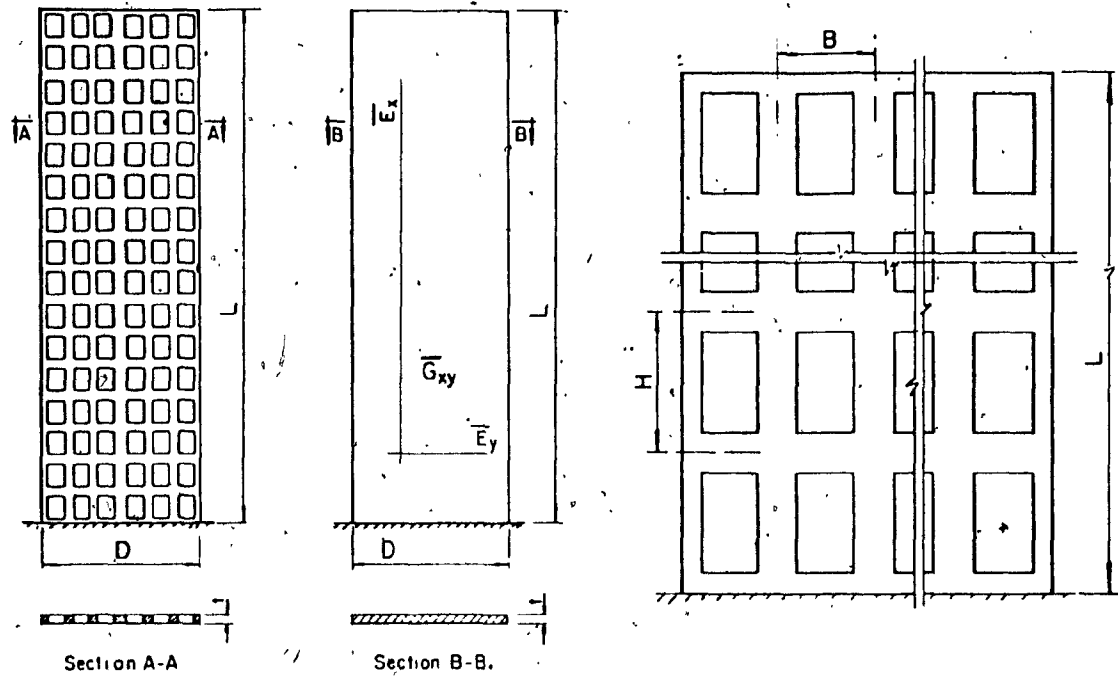
FIG. 1.2 - GEOMETRY OF A WALL-FRAME, [22]
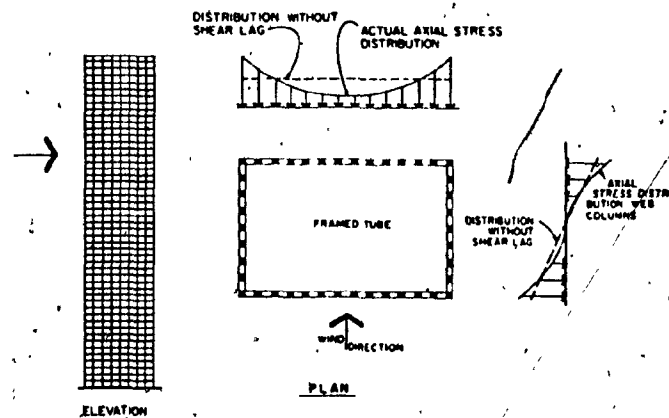
FIG. 1.3 - SHEAR LAG EFFECT, [9]

These considerable member sizes result in finite size joints giving the facade the appearance of a perforated wall rather than that of a frame. This type of facade is sometimes referred to as a wall-frame. An advantage of the wall-frame is developed by placing the windows directly into the framework. The need of an independent window wall system is thus done away with. Member proportioning can therefore be determined not only by structural requirements but also by the amount of desired glazed area on the facade.

Since interior floor girders are not required to participate in resisting lateral loads in the framed tube system, thin floor sandwich construction is often used.

1.3- BEHAVIOURAL CHARACTERISTICS OF FRAMED TUBE SYSTEMS

Framed tube structures are basically composed of a set of rigidly joined frame panels forming a tube in plan. This structural arrangement is particularily efficient because it utilizes all the buildings facades and available depth for resisting lateral loads.

The usual plane frame shearing action is converted into a more efficient cantilever tube bending action. This is attained by the transfer of lateral forces through the floor diaphragms directly to the walls of the tube.

The 3-dimensional behaviour of the framed tube system subjected to lateral forces may be better described as a

combination of two simpler dominant behavioural modes. The first is a cantilever bending mode where the lateral stiffness is provided by the frames normal to the direction of applied forces, by axial deformation of the columns and by their out-of-plane bending. The second is the usual frame shear deformation mode of the parallel frames which cause bending in the beams and columns.

The facades of the framed tube, due to their considerable member sizes, have the characteristic behaviour of both solid walls and plane frames. Perforated walls with small openings result in a predominantly bending type of behaviour, whereas walls with larger openings result in more dominant shearing action.

These perforations make the structure less stiff than the solid tube. In contrast with the pure bending behaviour of an ideal tube which exhibits a linear variation of the axial stress, the flexibility of the spandrel beams results in a non-linear stress distribution where higher axial forces occur in the corner columns and less in the center columns (Fig. 1.3).

This so called "shear lag effect" is mainly a function of the relative stiffnesses of the spandrel beams. Their flexibility tends to decrease the shear transfer between adjacent columns. Shear lag effect is also a function of the building's aspect ratio which directly determines the shear to bending mode type of deformations.

The non-linearity of axial force distribution may cause

warping of the floor slabs with consequent deformation of the interior partitions and secondary structure. The facades are thus designed to provide small shear flexibility to minimize this shear lag effect.

Rigid diaphragm action is achieved by the floor slabs interconnecting the tube facades. The large in-plane shear stiffness of the slab assures that differential lateral displacement of the individual frames and columns is negligible. The floor diaphragms thus provide lateral support to the columns at each floor level [5,14].

1.4- ANALYSIS METHODS

A typical framed tube structure may consist of thousands of rigidily connected members. Conventional computer analyses of such a system often involve a very high number of degrees of freedom (DOF). Sophisticated 3-dimensional analysis to account for the tube action is possible but complex. Computation time and the necessary memory requirements render the analysis very costly and the data preparation tedious. The problem is aggravated when non-linear dynamic and stability analyses are required.

A 3-dimensional analysis should also recognize the dual behaviour of the facades. Frame dominant wall-frame panels may be adequately analysed by using a standard plane frame analysis routine, using either centerline dimensioning or

using rigid-arms to simulate the finite size joints. But when the wall-frame is predominantly wall-like, the flexibility in the finite size joint should be considered in the analysis.

Thus simpler methods, specially for preliminary design purposes such as for assessing the structural behaviour or for preliminary member size evaluation, are definitely of interest. The main objectives would be to reduce computation time, memory requirements and to avoid lengthy data preparation while maintaining reasonable accuracy.

In the following sections, several simple analysis methods are briefly described in order to set up the proper background for the present work.

1.4.1- EQUIVALENT PLANE FRAME METHOD

The simplest approximate method consists in modelling the framed tube as an equivalent plane frame as shown in Fig. 1.4. Coull & Subedi,[7] and Khan & Amin,[16] have demonstrated that by recognizing the dominant mode of behaviour, the 3-dimensional problem can be treated as an equivalent plane frame thus reducing the computational effort.

In the method, the side and normal frames are modelled as lying in the same plane. The interaction between the frames is handled by coupling the vertical displacements
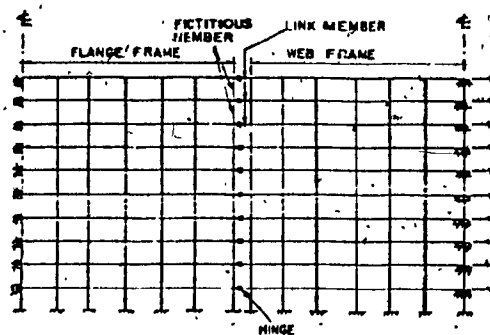
FIG. 1.4 - EQUIVALENT PLANE FRAME, [16]
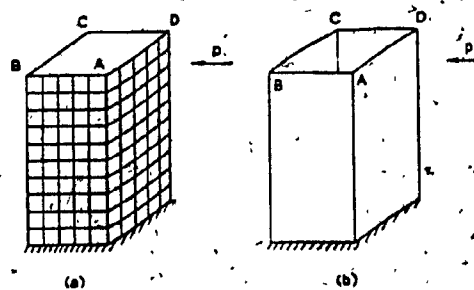
FIG. 1.5 - REAL AND SUBSTITUTE STRUCTURES, [5]

along the common edge thus producing a vertical shear transfer.

The main set-back to the method is the inadequate modelling of the flexibilty of the finite size joint. Since one of the primary characteristics of framed tube structures is large members and huge joints, modelling using centerline dimensions underestimates the lateral stiffness significantly. On the other hand, simulating the finite size joint with rigid arms considerably overestimates the lateral stiffness. The latter approach has been shown' to underestimate the maximum deflection by as much as 50 percent [1,17].

Despite of the simplification from a 3-D system to a 2-D system, the number of degrees of freedom is still quite large. This method is further restricted to buildings where torsion of the tube can be neglected.

1.4.2 CONTINUUM ANALOGY

Another dominant approach is by using energy methods. [2,5,10,12,15,17,18,21,22]. Most of these methods consist in replacing the beam-column grid system and any band of lintel beams by membranes with equivalent elastic properties. The problem is then reduced to analysing a substitute closed tube structure (Fig. 1.5). Closed form solutions are then obtained by means of energy methods.

These analytical solutions are often limited to systems with rectangular shapes of constant material properties and subjected to specific loadings. The assumed stress or displacement functions arrived in the solutions can be inadequate for high stress gradients associated with severe shear lag.

1.4.3- EQUIVALENT ORTHOTROPIC MACROELEMENT METHOD

Similar to the above technique of continuum analogy, this method replaces the discrete framework of beams and columns and any band of lintel beams by an elastically equivalent orthotropic membrane. The membrane is then rediscretized into macroelements, which may span over several storeys and bays, and analysed for displacements and stresses. From the condition of elastic equivalence, the displacements directly represent those of the actual structure and the member internal forces are obtained by integrating the corresponding stress components. The method has been shown to be quite accurate while requiring only a fraction of computation time, for both static and dynamic analyses [21,23].

This analysis approach is suitable for two main types of structures. Shear walls, coupled shear walls and core supported structures belong to the first category. The second type is basically any planar or tubular structure

- 12 -

composed of a rigidly connected gridwork of beams and columns. This macroelement analysis of an equivalent orthotropic membrane also applies to any planar frame/shear wall assembly.

Moselhi's "Equivalent Orthotropic Macroelement Method" [21] adopted in this study, is an approximate technique for elastic, static, and stability, analysis of framed tube structures. Moselhi's computer program named TUBE is capable of analysing multi-storey, multi-bay frames having a wide range of aspect ratios and stiffnesses, coupled shear walls, clad frames, planar and tubular structures consisting of frame and shear wall assemblies, and core-supported structures.

Moselhi's work was later extended by Mule [23] for dynamic analysis. The TUBE program was then modified for natural frequency calculations and earthquake spectral analysis.

Two plane stress finite elements (simple and refined), based on a displacement formulation, were developed by Moselhi for this macroelement technique. His simple 6-DOF element proved to be useful in the analysis of many tube-like buildings subjected primarily to shear mode deformations. However, it gave erroneous results when bending deformations became significant. This occurs when the aspect ratio of a frame facade is high or where there are tall shear/corewalls.

Furthermore, Moselhi's simple linear element was unable

- 13 -

to depict the non-linear variation of axial forces associated with shear lag. A refined 9-DOF element was thus developed and subsequently adopted for both static and dynamic analyses. This refinement, unfortunately, increased computation time and memory requirements significantly.

The incapability of Moselhi's simple element to depict bending behaviour, and the increased burden caused by his refined element prompted the work of this study. This study focuses on the development of improved, better suited plane stress finite elements for this macroelement technique.

These new elements specifically designed for bending behaviour, also behave well when a shear mode of deformation is dominant. Their applicability therefore cover both predominantly bending action components such as shear/corewalls and dominating shearing action characteristic to most planar frames.

1.5- OBJECTIVES OF THE STUDY

The primary objective of this work is to develop simple plane stress finite elements specifically for tall building analysis with greater applicability than the existing ones. To achieve this the elements should have the following characteristics. :

- good bending behaviour for the analysis of tall

- 14 -

building systems.

- rapid convergence property so that a coarse mesh such as in the macroelement technique can be used with confidence.

1.6- ORGANIZATION OF THESIS

For sake of completeness, the salient features of the the macroelement technique are presented in Chapter II.

In chapter III, specific finite elements for the macroelement technique are presented. Special attention is given in presenting two new strain based finite elements. The characteristics and convergence properties of these new elements are then investigated.

Chapter IV demonstrates the applicabilty of the two new elements for both static and dynamic analyses of planar frames and tubular structures.

In Chapter V, the weaknesses of the macroelement technique together with suggestions for improvement are outlined.

CHAPTER II

THE MACROELEMENT TECHNIQUE

FOR TALL BUILDING ANALYSIS

2.1- GENERAL ASSUMPTIONS

The following general assumptions are adopted in the present work:

1- The material is isotropic, homogeneous and linearly elastic.

2- Frame members form an orthogonal grid system.

3- All connections are rigid.

4- Small perforation ratios.

5- Inflection points situated at mid-span of all members.

6- In-plane deformations of floor diaphragms are negligible.

7- Out-of-plane deformations of facades (& members) can be ignored.

Most of the above assumptions are commonly adopted in the analysis of tall building structures subjected to lateral loading.

2.2- ORTHOTROPIC MEMBRANE FOR COUPLING BEAMS

Consider the coupled shear walls whose band of lintel beams are to be replaced by an equivalent lamina of Fig. 2.1. This planar system could be part of a 3-dimensional corewall assembly.

The elastic properties of the equivalent membrane are derived on the principle of elastic equivalence. Both shear and bending deformations in the coupling beams are considered in order to cover a wide range of coupling elements (i.e., from slabs to deep lintel beams).

Consider the coupling element of Fig. 2.2, where a point of contraflexure is assumed at half-span. This common assumption has been used by many authors' and shown to be quite acceptable [3,6,13,25]. The maximum deflection due to both bending and shear deformations in the coupling element is equated to the shear deflection in the membrane yielding an expression for the equivalent shear modulus, [21]:

$$\overline{G}_{xy} = \frac{E/tH}{(L^2/12I + E/GA_r)} \qquad (2.1)$$

in which:

E, G = elastic modulii of lintel beam material.

I, A_r = moment of inertia and reduced (effective) shear area of beam cross-section.

L = span of lintel beam.

H = storey height.

- 17 -

(a) ACTUAL STRUCTURE   (b) EQUIVALENT STRUCTURE
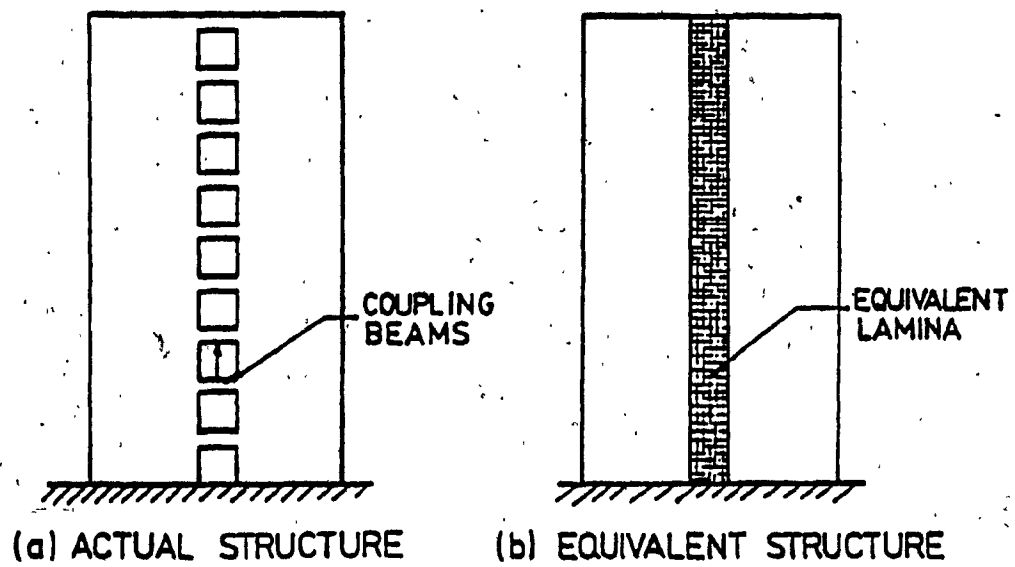
FIG. 2.1 - MODELLING OF COUPLED SHEAR WALL, [21]
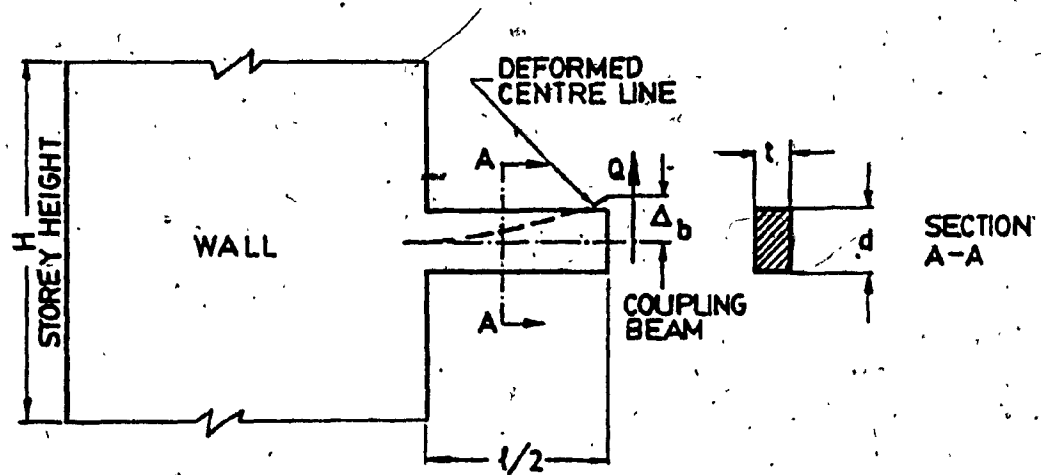
(a) ACTUAL STRUCTURE
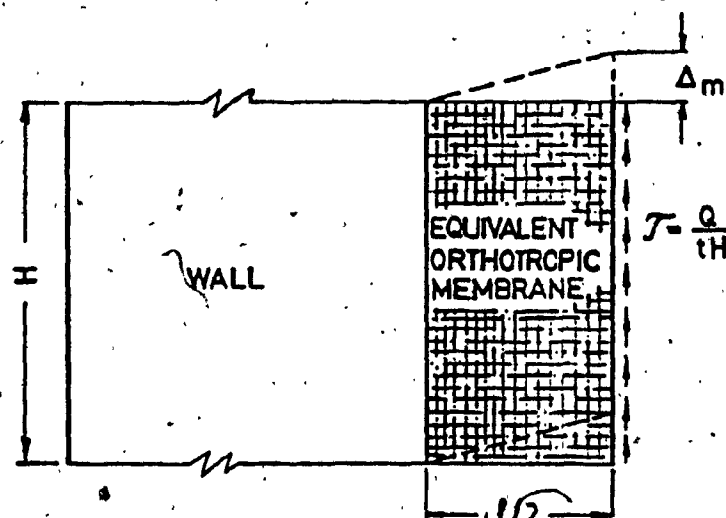
(b) EQUIVALENT STRUCTURE

FIG. 2.2 - MODELLING OF COUPLING BEAMS, [21]

t   = thickness of membrane.

If the coupling element is a rectangular beam of thickness t and depth d, the shear modulus $\overline{G}_{xy}$ can be expressed as, [21]:

$$\overline{G}_{xy} = \frac{E(d/H)}{[(L/d)^2 + 1.2 (E/G)]} \tag{2.2}$$

2.3- ORTHOTROPIC MEMBRANE FOR PLANAR GRIDWORK SYSTEM

In modelling the discrete beam-column system of a framed tube by an equivalent orthotropic membrane, the large member sizes must be recognized. Thus, in addition to the bending and shear deformations, the flexibility of the finite size joints should be considered in evaluating the equivalent elastic properties. If the structure is being analysed for gravity loading, the reduction of member stiffnesses due to axial loads, and the P-Δ effect must also be considered.

Consider a rectangular segment of a grid system, composed of beams and columns and bounded by four inflection points (Fig. 2.3). This segment is to be modelled by an equivalent membrane spanning the same area. The elastic properties of the membrane are derived on the basis that under a set of statically equivalent external forces, both the actual grid and membrane units shall develop the same

characteristic   deformations.   In   evaluating   these
deformations, the flexibilty of the finite size joints are
assessed in addition to bending and shear deformations.

2.3.1- MODULUS $\overline{E}_y$

To derive the modulus of elasticity $\overline{E}_y$ of the
equivalent membrane, a vertical force P is applied on the
grid segment (Fig. 2.3). The vertical displacement of the
grid unit is equated to the vertical displacement of the
membrane yielding an expression for the elastic modulus of
the equivalent membrane $\overline{E}_y$, [21]:

$$\overline{E}_y = \frac{E\, t_c\, d_c}{t_b\, B\, C_y} \qquad (2.3)$$

in which:

$$C_y = 1 - \frac{d_b}{H} + \frac{t_b}{t_b}\left[\frac{d_b d_c}{BH} + \frac{8B}{\pi^4 H}\cdot\frac{1}{3}\sum_{n=1}^{3}\sum_{m=1}^{\infty}\frac{A_m A_n}{m}Sinh^2\alpha\, d_b\right] \qquad (2.4)$$

where:

$$A_n = COS\,\alpha\, d_c\,(2-n)$$

$$A_m = \frac{SIN\,\alpha\, d_c}{m(SINH\, 2\alpha\, d_b + 2\alpha\, d_b)} \qquad (2.5)$$

$$\alpha = m\pi/B$$

d_c , t_c = column depth and thickness respectively.
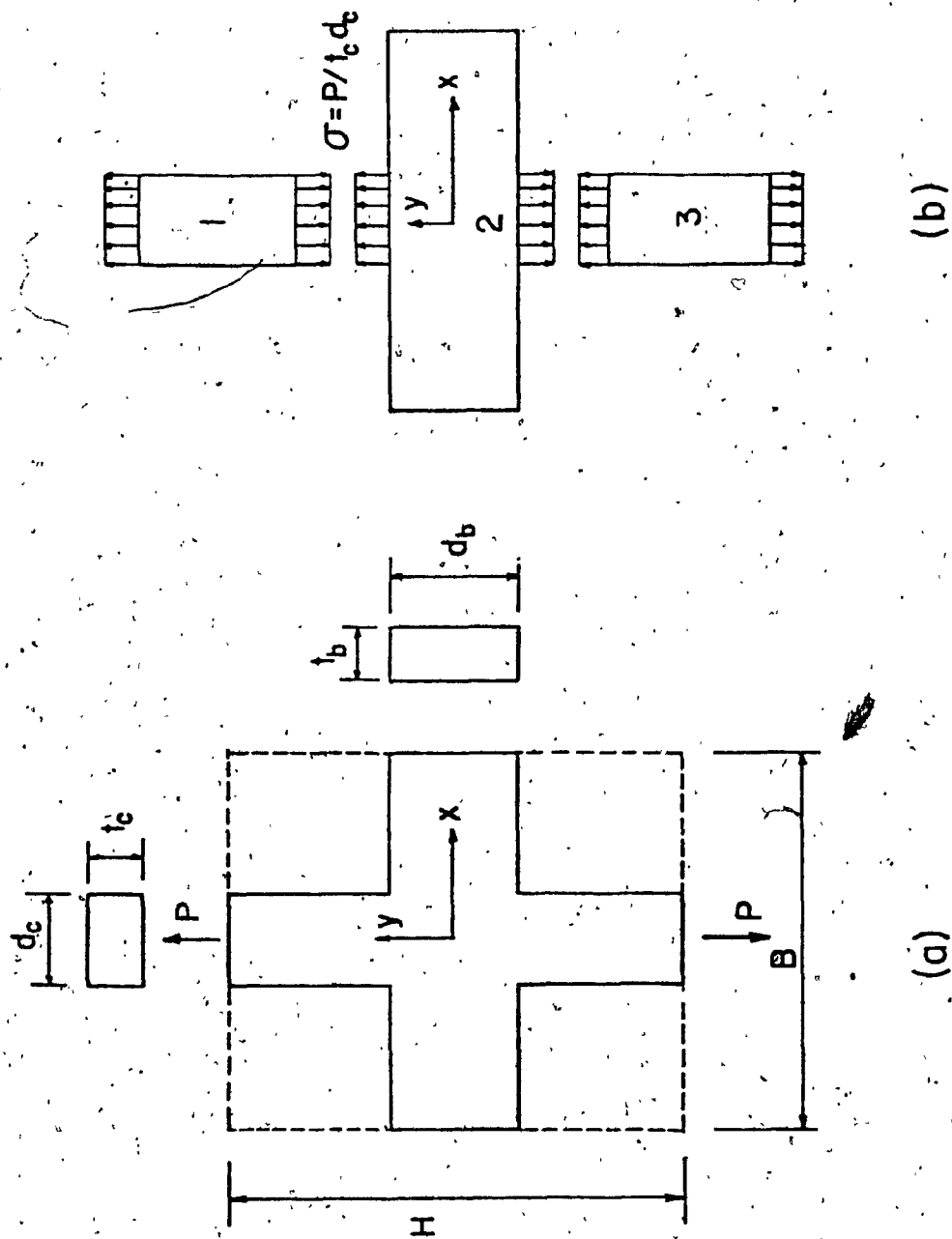
FIG. 2.3 — MODEL FOR EVALUATING EQUIVALENT ELASTIC MODULUS $\overline{E}_y$, [21]

d_b , t_b = beam depth and thickness respectively.

    B   = bay width

    H   = storey height

Note that the vertical displacement of part 2 in Fig. 2.3b) was obtained by theory of elasticity solution. Further note that this expression is only valid for a concrete beam-column unit since the stress path around the joint would differ in a steel unit.

An equivalent elastic modulus $\overline{E}_x$ can be derived in a similar manner. However it is not required because the floors are considered as rigid diaphragms.

2.3.2- MODULUS $\overline{G}_{xy}$

The same unit is now subjected to a horizontal force Q (Fig. 2.4). The total lateral displacement in the grid unit is obtained by considering shear and bending deformations in both beams and columns together with the shear deformations within the finite size joint. Equating this displacement to that of the membrane subjected to an equivalent force yields an expression for the shear modulus of the equivalent membrane $\overline{G}_{xy}$,[21]:

$$\overline{G}_{xy} = \frac{E}{t_b \; B \; C_{xy}}$$
(2.6)
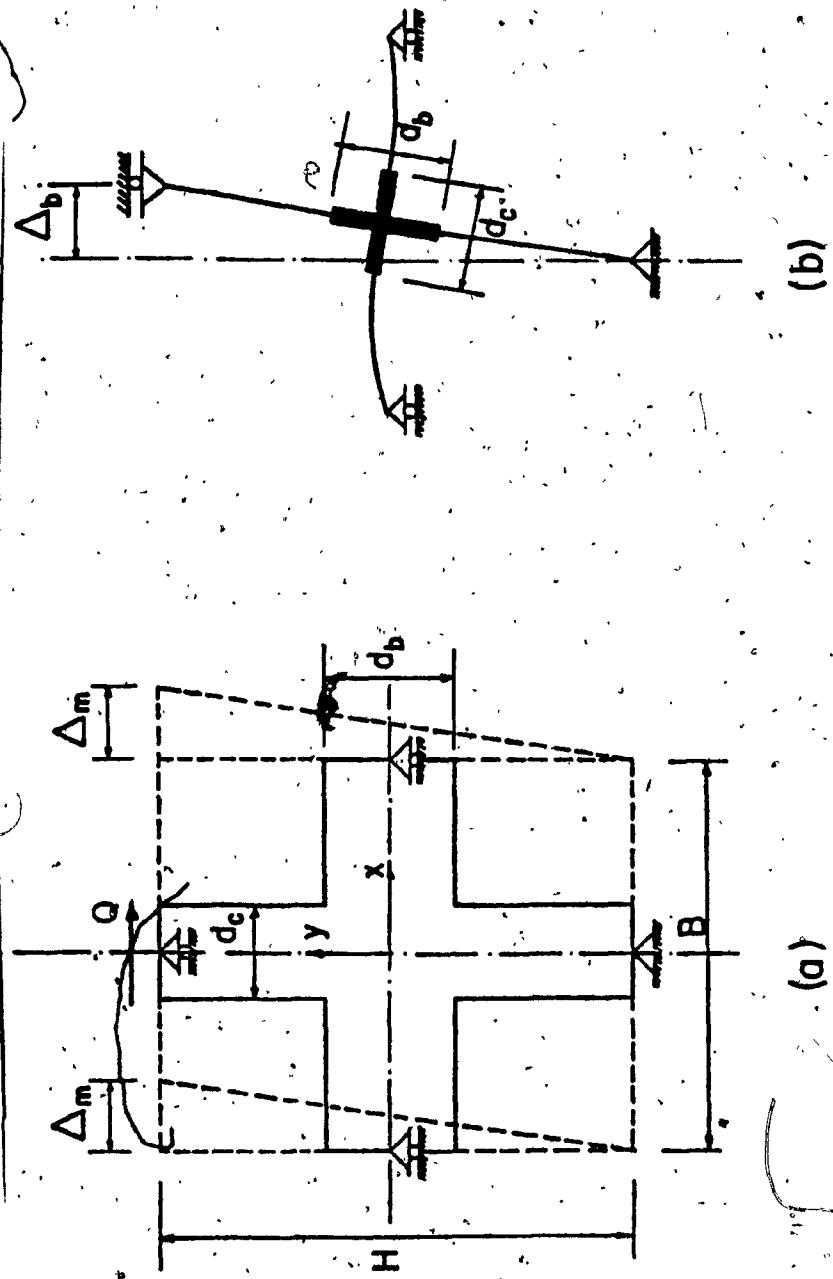
FIG. 2.4 - MODEL FOR EVALUATING EQUIVALENT SHEAR MODULUS $\overline{G}_{xy}$ [21]

in which:

$$C_{xy} = \frac{(H-db)^3}{12HI_c} + \frac{H(B-d_c)^3}{12B^2 I_b} + \frac{E}{G}\left[\frac{H(B-d_c)}{B^2 A_{rb}} + \frac{H-db}{H A_{rc}} + \frac{H}{A_{rj}db}\left(1-\frac{d_c}{B}-\frac{db}{H}\right)^2\right]$$

(2.7)

where:

I_b , Ic = moment of inertia of beam and column respectively.

A_{rb} , Arc , = effective shear area of beam, column
A_{rj} and joint respectively.

G = shear modulus of actual structure.

For a steel unit, a similar expression could be obtained by considering the so called "panel-zone deformations" to account for the flexibility within the finite size joint.

2.3.3- SECOND-ORDER EFFECTS

Frames subjected to combined gravity and lateral loads are significantly affected by a P-Δ moment resulting from the gravity loads P in going through a sway Δ. This secondary effect generally produces an increase in stress and displacements, which can be very significant for tall buildings. To account for this effect the shear modulus $\overline{G}_{xy}$ of the membrane is reduced to $\overline{G}_{xy}$ and the lateral load Q is magnified to $\overline{Q}$. These amplification factors are given by, [21]:

- 25 -

$$\overline{G}_{xy} = G_{xy} \left\{ \frac{1 + \left(\frac{I_c \ell_b}{I_b \ell_c}\right)}{\left(\frac{30-5\alpha^2}{30-7\alpha^2}\right) + \left(\frac{I_c \ell_b}{I_b \ell_c}\right)} \right\}$$

(2.8)

$$\overline{Q} = Q \left\{ \frac{1}{1 - \left(\frac{P}{\ell B G_{xy}}\right)} \right\}$$

in which:

$$\alpha = H\sqrt{P/EI}$$

2.4- THE MACROELEMENT TECHNIQUE

Once the properties of the substitute structure are determined, the structure is discretized into macroelements. The term "macro" is used here instead of "finite" because an element may encompass several bays and stories. A finite element on the other hand, signifies a discretization into small parts. But strictly speaking, since we are talking about discretization of a-membrane with uniform properties rather than of a framework of beams and columns, the term "finite" can equally be used.

The complete structure is first replaced by a set of equivalent orthotropic membranes. Each membrane may represent a tube facade; a band of lintel beams, or a face of a supporting core. The membranes are then discretized into a set of rectangular macroelements, interconnected at

the nodes. The equivalent structure is subsequently analysed for the nodal displacements and stresses.

The internal displacements of a macroelement, obtained by the elements shape functions, represent the actual displacements of the members and joints. Thus, formulation of the shape functions requires special attention. In the next chapter, four finite elements particularly suited for tall building analysis are presented.

2.4.1- INTERNAL MEMBER FORCES

Once the equivalent structure has been analysed for nodal displacements and stresses, the internal member forces can be determined. The procedure for approximating these internal member forces as described in this section is taken from Moselhi's TUBE program [21].

First, stresses in the equivalent membrane are determined along the beam and column lines. From the condition of elastic equivalence, these stresses are converted into member stresses from which internal member forces are determined. The exact procedure is described in more detail in the following two sections.

2.4.1.1- COLUMN INTERNAL FORCES

Consider the grid unit and its equivalent membrane subjected to an axial force P in Fig. 2.5a. The force P produces an axial stress σ_{cy} in the column of the grid unit and an axial stress σ_{my} in the membrane. Therefore:

$$\sigma_{cy} \cdot A_c = \sigma_{my} \, A_m \tag{2.9}$$

where:

A_c = column cross-sectional area. ___

A_m = membrane " " .

If t_e is the column thickness, and d_c the column depth, and if B and t_m are the bay width and membrane thickness respectively (Fig. 2.5a), then Eq. (2.9) can be rewritten as:

$$\sigma_{cy} = \frac{B \, t_m}{d_c \, t_c} \, \sigma_{my} \tag{2.10}$$

Eq. (2.10) relates the axial stress in the membrane along a column line to the axial stress in the column. The axial force in the column is thus simply:

$$P = \sigma_{cy} A_c = \sigma_{my} B \, t_m \tag{2.11}$$

Using a similar approach, the column shear force V_c is obtained from the shearing stress in the equivalent membrane
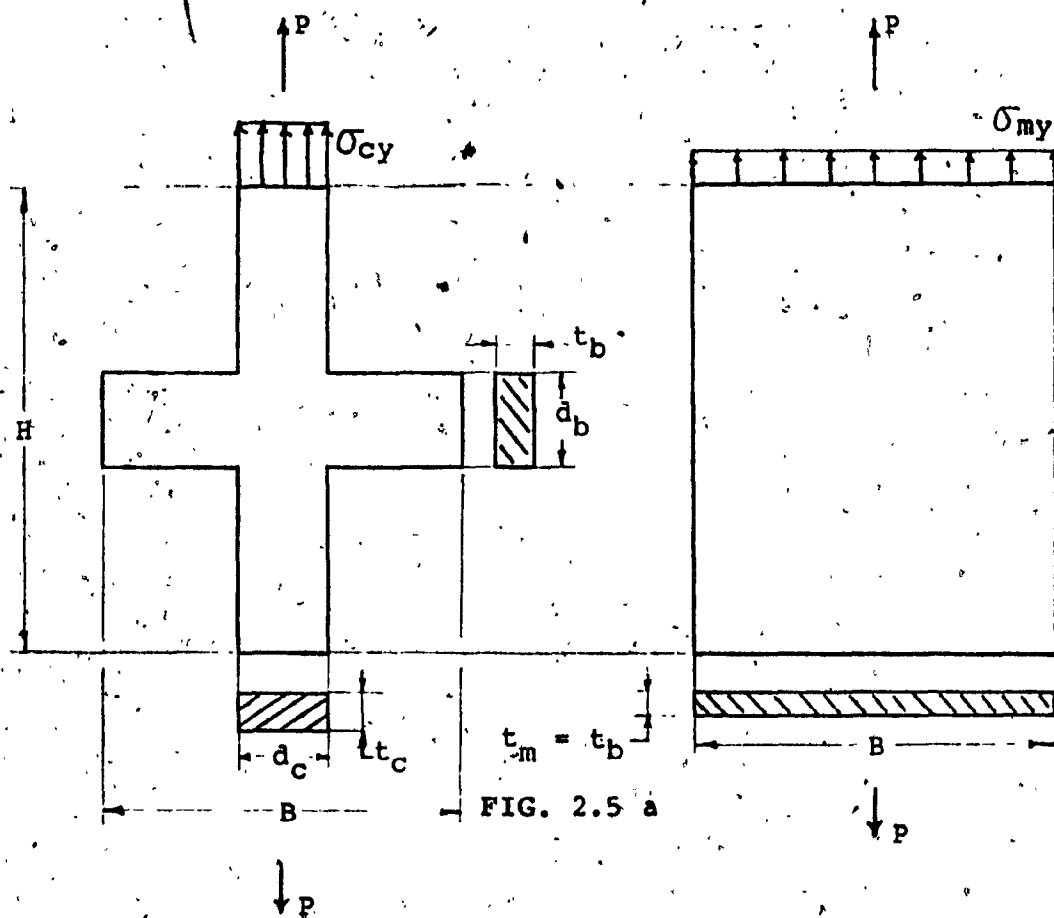
FIG. 2.5 a
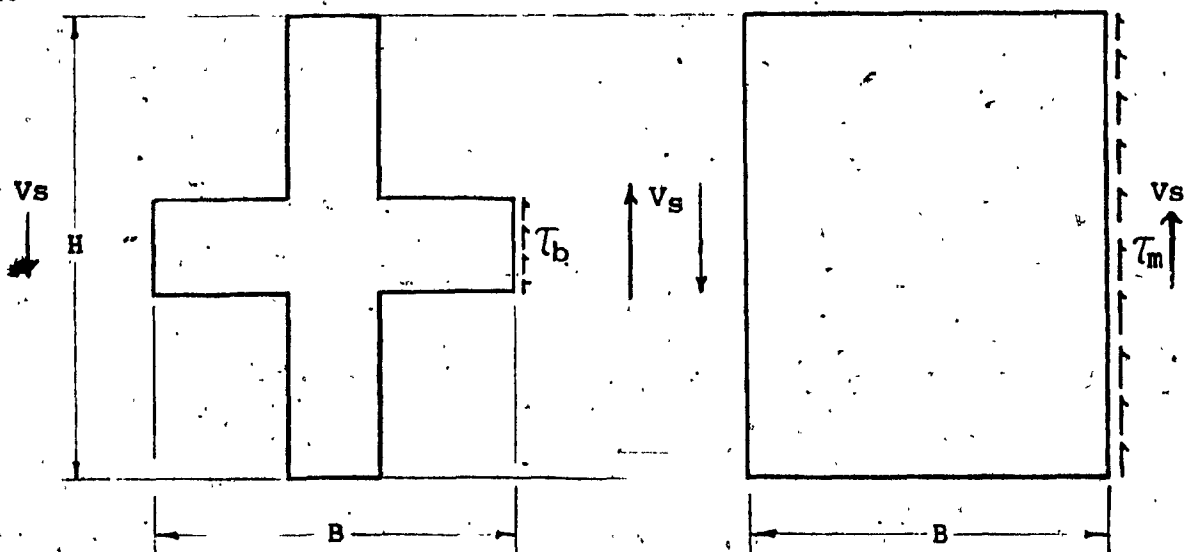
FIG. 2.5 b

FIG. 2.5 - MODELS FOR DETERMINING INTERNAL MEMBER FORCES

- 29 -

along a column line:

$$V_c = \mathcal{T}_m \, B \, t_m \qquad\qquad (2.12)$$

where $\mathcal{T}_m$ is the shearing stress in the equivalent membrane along a column line. The bending moment, M_c in the column is then simply determined by multiplying the shear force by half the storey height, H:

$$M_c = V_c \, H/2 \qquad\qquad (2.13)$$

2.4.1.2- BEAM INTERNAL FORCES

Consider the grid unit, and its equivalent membrane subjected to a shear force V_s in Fig. 2.5b. The shear force V_s produces a shearing stress $\mathcal{T}_b$ in the beam and a shearing stress $\mathcal{T}_m$ in the membrane. Therefore:

$$\mathcal{T}_b \, A_b = \mathcal{T}_m \, A_m \qquad\qquad (2.14)$$

where:

A_b = beam cross-sectional area.

A_m = membrane   "   " .

If the beam is of depth d_b and thickness tb and if H is the storey height (Fig. 2.5b), then Eq. (2.14) may be rewritten as:

$$\tau_b = H\,\tau_m\,/d_b \qquad\qquad (2.15)$$

Eq. (2.15) gives the relationship between the shearing stress in the membrane along a beam line and the shearing stress in the beam. Note that the membrane thickness is taken as the beam thickness. The shearing force V_b in the beam is then simply given by:

$$V_b = \tau_b\,A_b = \tau_m\,H\,t_m \qquad\qquad (2.16)$$

and the bending moment M_b in the beam, by:

$$M_b = V_b\,B/2 \qquad\qquad (2.17)$$

CHAPTER III

SPECIFIC FINITE ELEMENTS FOR
TALL BUILDING ANALYSIS

3.1- INTRODUCTION

In this chapter, four finite elements specifically for tall building analysis are presented. Two of these, were presented by Moselhi [21], and the other two are developed in the chapter.

The four elements are specific to tall building analysis because they are formulated to incorporate the assumption of infinite in-plane rigidity of floors. This well accepted assumption for tall building analysis, was shown by Moselhi to be equally acceptable in the analysis of tube-like structures. The assumption allows for a considerable reduction in computation without any significant loss in accuracy.

The two elements developed by Moselhi [21], were based on the displacement formulation: one with 6 degrees of freedom (6DOFD) and the other with 9 degrees of freedom (9DOFD). Note that the letter 'D' attached at the end of the element designation indicates the displacement formulation. The elements to be derived in the present study are obtained from a "strain based" formulation, thus their designation has the letter 'S' attached. Advantages

of these strain based elements will be made clear in the later sections.

For the ease of presentation, the elements are classified as simple elements (6DOFD & 6DOFS) and refined elements (9DOFD & 8DOFS) purely on the basis of the number of degrees of freedom. They are grouped as such so that comparisons can be fairly made between the displacement and strain based elements possessing a similar number of degrees of freedom.

The four elements are now presented briefly with special attention being paid on the formulation of the strain based finite elements. Testing of the elements will then show the characteristics of the strain based elements in contrast to those of the displacement based elements.

3.2- SIMPLE ELEMENTS

3.2.1- 6DOFD DISPLACEMENT BASED ELEMENT

Consider the rectangular 4 node, 6 DOF element of Fig. 3.1. In accordance with the assumption of rigid floors, the strain in the x-direction, ϵ_x is neglected.

The displacement functions that maintain compatibility along the edges and that satisfy the convergence criteria are given by, [21]:

$$\overline{X} = X/a \quad \overline{Y} = Y/b$$
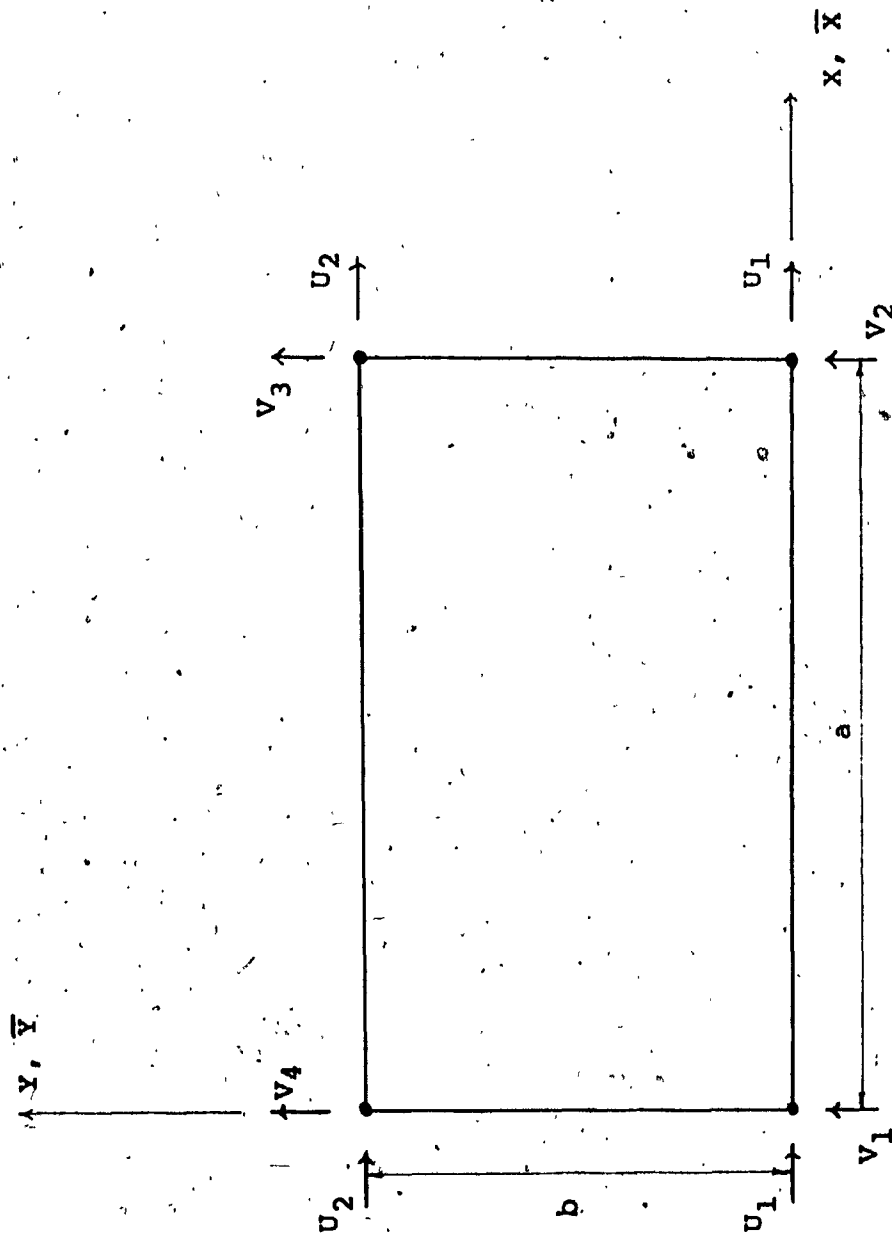
FIG. 3.1 - SIMPLE 6-DOF ELEMENT

$$\begin{cases} U = A_1 + A_2 \,\overline{Y} \\ V = A_3 + A_4 \,\overline{X} + A_5 \,\overline{Y} + A_6 \,\overline{X}\,\overline{Y} \end{cases} \tag{3.1}$$

where $\overline{X}$ and $\overline{Y}$ are non-dimensional coordinates equal to X/a and Y/b respectively (Fig. 3.1). These displacement functions are the simplest that can be designated to this 6-DOF element. The corresponding strain variations will be examined in Section 3.2.3. The 6x6 element stiffness matrix of the 6DOFD element based on the above displacement formulation is obtained as, [21]:

$$[\,K\,] = \begin{bmatrix} K1 & & & & & \\ -K1 & K1 & & & \text{SYMM.} & \\ K2 & -K2 & K3 & & & \\ -K2 & K2 & K4 & K3 & & \\ -K2 & K2 & -K3/2 & K5 & K3 & \\ K2 & -K2 & K5 & -K3/2 & K4 & K3 \end{bmatrix}$$

in which:

$$K1 = taG_{xy}/b \tag{3.2}$$

$$K2 = tG_{xy}/2$$

$$K3 = t(E_y\, a/b + G_{xy}\, b/a)/3$$

$$K4 = t(E_y\, a/2b - G_{xy}\, b/a)/3$$

$$K5 = t(G_{xy}\, b/2a - E_y\, a/b)/3$$

where:

a,b = are the width and height of the element.

t = thickness of the membrane (taken as the beam thickness).

E_y , G_{xy} = modulii of the material.

3.2.2- 6DOFS STRAIN BASED ELEMENT

The main objective of this section is to create an element which will be able to describe both the shear and bending behaviour better than that of the 6DOFD element without having to go to a higher order element. The strain rather then displacement approach will be used here. The 6DOFS element, where the 'S' signifies based on an assumed strain field is a modified form of Sabir's 8 DOF SBRIE element [24].

Consider the same 4 node, 6 DOF, rectangular element (Fig. 3.1). The assumed displacement functions should have the following desirable properties:

1- Infinite in-plane rigidity of floors (E_x = inf., ϵ_x =0).
2- Strain-free rigid body displacement motion.
3- Compatibility within the element.
4- Realistic strain distribution corresponding to bending behaviour.

These displacement functions will be obtained by considering the strain variation associated with the bending behaviour. Consider the following strain-displacement relationships:

$$\begin{cases} \epsilon_x = \partial U/\partial X \\ \epsilon_y = \partial V/\partial Y \\ \gamma_{xy} = \partial U/\partial Y + \partial V/\partial X \end{cases} \qquad (3.3)$$

Equating the above set of equations to zero and integrating, the simplest displacement functions associated with rigid-body motions are obtained as follows:

$$\begin{aligned} U &= A_1 - A_3 Y \\ V &= A_2 + A_3 X \end{aligned} \qquad (3.4)$$

The shape functions for the desired 6DOFS element should contain 6 independent constants (A_i). Having used 3 constants to describe the rigid-body motions, we are left with 3 constants to represent the straining/deformation behaviour of the element. Let them be distributed as such:

$$\begin{cases} \epsilon_x = 0 \\ \epsilon_y = A_4 + A_5 X \\ \gamma_{xy} = A_6 \end{cases} \qquad (3.5)$$

Note that these strain variations describe a pure bending state. The first of Eqs. (3.5) represents the rigid floor diaphragm assumption, the second a linear variation of strain in the y-direction and the third an independent constant shearing strain. Compatibility of strains within the element as exemplified by the equation:

$$\frac{\partial^2 \gamma_{xy}}{\partial x \partial y} = \frac{\partial^2 \epsilon_x}{\partial y^2} + \frac{\partial^2 \epsilon_y}{\partial x^2} \qquad (3.6)$$

is identically satisfied.

By equating the strain expressions of Eq. (3.5) to the strain-displacement relationships of Eq. (3.3) and integrating, the corresponding displacement functions are obtained.

The first two equations of (3.3) yield:

$$\begin{cases} U = C_1 \ (Y) \\ V = A_4 \ Y + A_5 \ XY + C_2 \ (X) \end{cases} \qquad (3.7)$$

where C_1 and C_2 are functions of Y and X respectively. The third equation of (3.3) gives:

$$\frac{dC_1}{dy} + \frac{dC_2}{dx} = -A_5 \ Y + A_6 \qquad (3.8)$$

Since C_1 is a function of Y only and C_2 of X only, it follows that:

$$\begin{cases} C_1 = -A_5 \ Y^2 \ /2 \ + \ A_6 \ Y \ /2 \\ C_2 := A_6 \ X/2 \end{cases} \qquad (3.9)$$

Thus Eqn. (3.7) becomes:

$$\begin{cases} U = -A_5 \ Y^2 \ /2 \ + \ A_6 \ Y/2 \\ V = A_4 \ Y + A_5 \ XY + A_6 \ X/2 \end{cases} \qquad (3.10a)$$

These are added to the displacement functions associated with the rigid-body displacement mode, Eqs. (3.4) to obtain the final displacement functions of the 6DOFS element:

$$
\left\{
\begin{array}{l}
U = A_1 - A_3 Y - A_5 Y^2/2 + A_6 Y/2 \\
V = A_2 + A_3 X + A_4 Y + A_5 XY + A_6 X/2
\end{array}
\right.
\tag{3.10b}
$$

These are the simplest displacement functions that contain only 6 displacement parameters and that satisfy the four desirable properties listed previously.

The displacement functions as defined by Eq. (3.10b) render the element non-conforming. That is to say, there is displacement incompatibility among adjacent elements along their edges. It is interesting to note where this incompatibility arises. Although the V-displacement function with its linear variation does not violate edge compatibilty, the U-displacement function exhibits a quadratic variation with only two horizontal DOF (U_1, U_2). Thus overlapping or separation of the vertical edges between two adjacent elements can occur.

The strain-displacement matrix is obtained from Eq. (3.3) as:

$$
\left\{
\begin{array}{c}
\epsilon_x \\
\epsilon_y \\
\gamma_{xy}
\end{array}
\right\}
=
\left[
\begin{array}{cccccc}
0 & 0 & 0 & 0 & 0 & 0 \\
0 & 0 & -(1-\overline{X})/b & -\overline{X}/b & \overline{X}/b & (1-\overline{X})/b \\
-1/b & 1/b & -1/2a & 1/2a & 1/2a & -1/2a
\end{array}
\right]
\left\{
\begin{array}{c}
U_1 \\
U_2 \\
V_1 \\
V_2 \\
V_3 \\
V_4
\end{array}
\right\}
$$

$$\tag{3.11}$$

or in symbolic form:

$$\{ \varepsilon \} = [B] \{ d \} \qquad (3.12)$$

where $\overline{X}$ is the non-dimensional coordinate equal to x/a (Fig. 3.1).

The corresponding 6x6 stiffness matrix is then obtained by carrying out the integration of the usual triple matrix product over the volume of the element:

$$[K] = \int_{vol} [B]^{T} [E] [B] \, dV \qquad (3.13)$$

Note that the matrix of elastic constants [E], becomes a diagonal matrix. This is due to the zero value assigned to the Poisson's ratio in accordance with the assumption of rigid floor diaphragm.

The stiffness matrix is then obtained as:

$$[K] = \begin{bmatrix} K1 & & & & & \\ -K1 & K1 & & & \text{SYMM.} & \\ K2 & -K2 & K3 & & & \\ -K2 & K2 & K4 & K3 & & \\ -K2 & K2 & K5 & K6 & K3 & \\ K2 & -K2 & K6 & K5 & K4 & K3 \end{bmatrix}$$

where:

$$K1 = taG_{xy} /b \qquad (3.14)$$

$$K2 = tG_{xy} /2$$

$$K3 = t(aE_y/3b + bG_{xy}/4a)$$

$$K4 = t(aE_y/6b - bG_{xy}/4a)$$

$$K5 = -t(aE_y/6b + bG_{xy}/4a)$$

$$K6 = -t(aE_y/3b - bG_{xy}/4a)$$

3.2.3- COMPARISON OF FORMULATIONS

The main difference in the formulation of the two simple elements is in the final assumed displacement functions. From then on, the derivation steps are identical.

On examining the displacement functions of the simple elements, one first notices that they are coupled in the case of the strain based element. This coupling has a certain effect on the strain distribution and element performance.

Upon differentiating Eq. (3.1), the strain variations in the displacement based 6DOFD element are obtained as:

$$\begin{cases} \varepsilon_x = 0 \\ \varepsilon_y = A_5 + A_6 X \\ \gamma_{xy} = A_2 + A_4 + A_6 Y \end{cases} \tag{3.15}$$

It is interesting to note here that the shearing strain is linked to the direct strain in the y-direction. This indicates that linear direct strain and an independent constant shearing strain required to simulate bending

- 41 -

behaviour cannot be attained with the 6DOFD element. (ie: $A_6 = 0$, giving rise to constant $\mathcal{E}_y$). Many authors refer to this shearing stress under pure bending as parasitic shear and outline that its unwanted stiffening effect can become severe with a high aspect ratio [4].

One may further look at the analytical solution of a pure bending state with Poisson's effect neglected as given by:

$$U = C - DY^2/2$$
$$V = DXY$$

$$(3.16)$$

where C and D are constants. The second equation corresponds to the assumption that plane sections remain plane after bending and the first equation gives the associated constant change in curvature. The strain based 6DOFS element possesses both these terms in its displacement functions whereas the displacement based 6DOFD element does not have the quadratic term to allow for a change in curvature.

Consider a beam segment subjected to pure bending, Fig. 3.2 a). The linear 6DOFD element cannot produce the curved edges needed for bending. Instead, the sides of the linear element remain straight causing the element to deform as shown in Fig. 3.2 b). As stated previously, the linear element gives rise to shearing stresses under pure bending. Thus not only do these elements offer bending resistance but also a shear resistance under pure bending. This anomaly
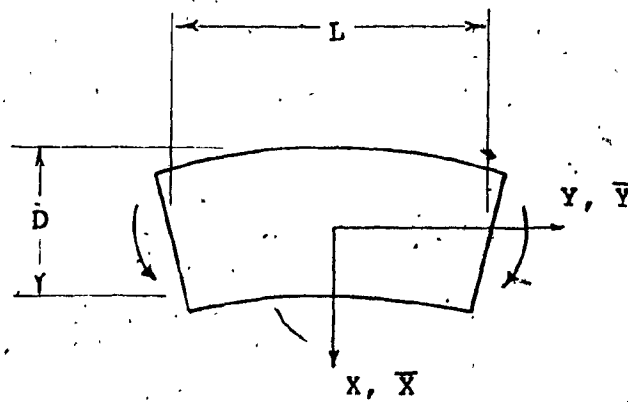
FIG. 3.2 a)
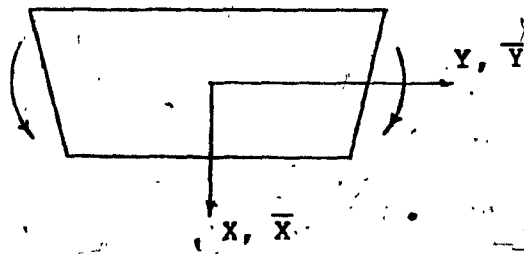
FIG. 3.2 b)

FIG. 3.2 - BEAM SEGMENT SUBJECTED TO PURE BENDING

render the displacement based element too stiff in a bending mode.

3.3- REFINED ELEMENTS

The term "refined element" is used here to refer to elements with more than 6 degrees of freedom. This type of higher order element is devised for the expressed purpose of improving the strain distribution and thereby, hopefully, improving the accuracy of the solutions. It would be worthwhile using the refined elements in preference over the simple elements if, for a comparable level of accuracy, a coarser mesh is sufficient.

In this section two elements are presented. The first is a 9-DOF element developed by Moselhi [21], based on a displacement formulation and the second is a new strain based 8-DOF element.

3.3.1- 9DOFD DISPLACEMENT BASED ELEMENT

Consider the rectangular 8 node, 9 DOF element of Fig. 3.3. A suitable displacement field which maintains compatibilty along the edges and that satisfies both the convergence criteria and the rigid floor diaphragm requirement is given by, [21]:

- 44 -
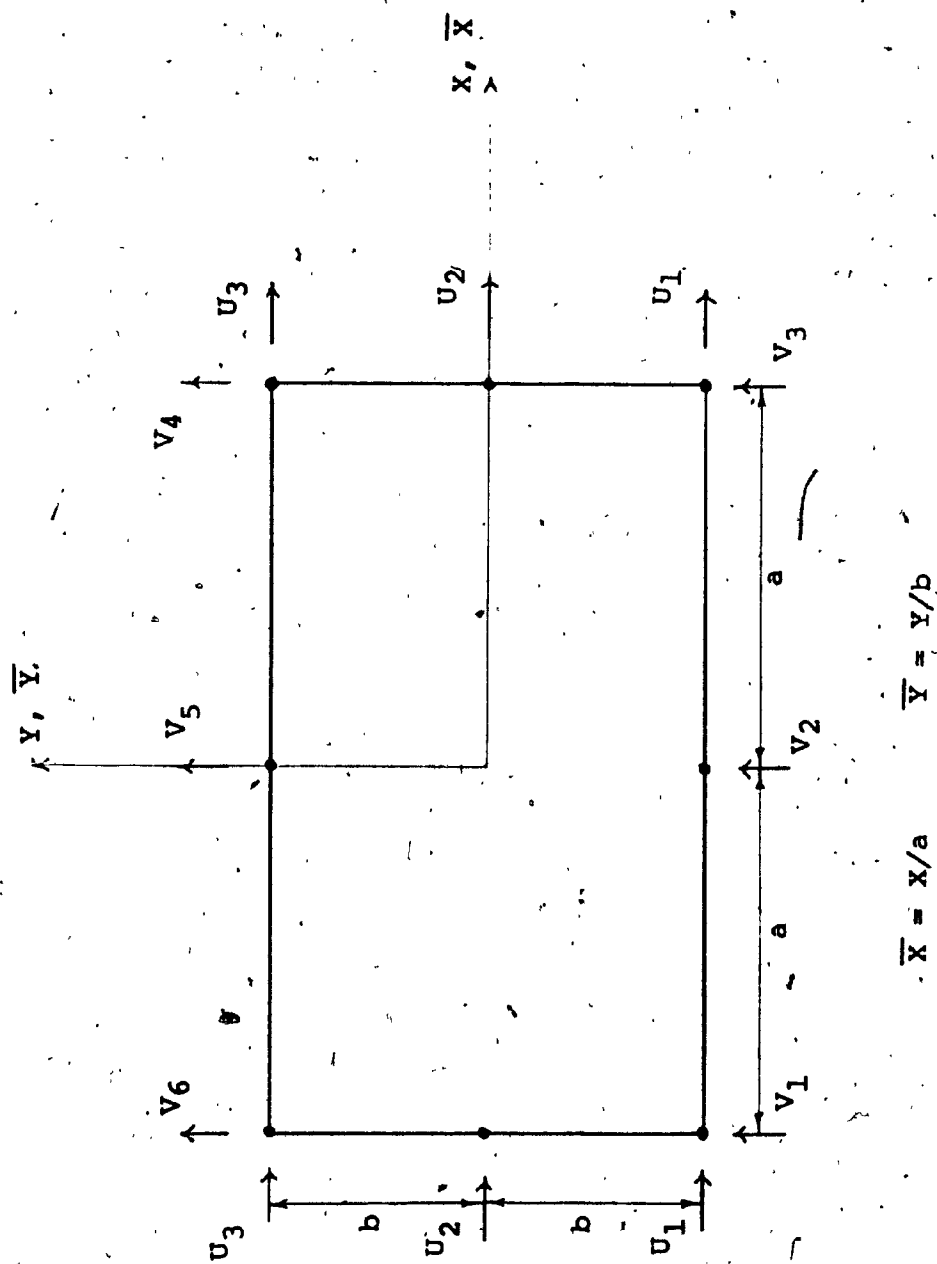
FIG. 3.3 — REFINED 9 DOFD ELEMENT

$$\overline{X} = X/a \qquad \overline{Y} = Y/b$$

$$\begin{cases} U = A_1 + A_2 \cdot \overline{Y} + A_3 \ \overline{Y}^2 \\ V = A_4 + A_5 \ \overline{X} + A_6 \ \overline{Y} + A_7 \ \overline{X}^2 + A_8 \ \overline{XY} + A_9 \ \overline{YX}^2 \end{cases} \qquad (3.17)$$

Note that the element is of length 2a and height 2b with the origin of the X and Y axis located at the center of the element (Fig. 3.3). The 9x9 element stiffness matrix is given as, [21]:

$$[K] = \begin{bmatrix}
7K1 & & & & & & & & \\
-8K1 & 16K1 & & & & & & & \\
K1 & -8K1 & 7K1 & & & \text{SYMM.} & & & \\
5K2 & -4K2 & -K2 & K3 & & & & & \\
0 & 0 & 0 & K4 & K9 & & & & \\
-5K2 & 4K2 & K2 & K5 & K4 & K3 & & & \\
-K2 & -4K2 & 5K2 & K6 & K7 & K8 & K3 & & \\
0 & 0 & 0 & K7 & K10 & K7 & K4 & K9 & \\
K2 & 4K2 & -5K2 & K8 & K7 & K6 & K5 & K4 & K3
\end{bmatrix}$$

in which:

$$K1 = trG_{xy} /3 \qquad (3.18)$$

$$K2 = tG_{xy} /6$$

$$K3 = t(2rE_y /15 + 7Gxy /9r)$$

$$K4 = t(rE_y /5 - 8Gxy /3r)/3$$

$$K5 = -t(rE_y /5 - 2Gxy /3r)/6$$

$$K6 = t(rE_y /5 + Gxy /3r)/6$$

$$K7 = -t(rE_y /15 + 4Gxy /9r)$$

$$K8 = -t(4rE_y /5 - 7Gxy /3r)/6$$

$$K9 = 8t(rE_y /5 + 2Gxy /3r)/3$$

$$K10 = -8t(rE_y /5 - Gxy /3r)/3$$

where: r = element aspect ratio = a/b

3.3.2- 8DOFS STRAIN BASED ELEMENT

In this section a strain based higher order element, good in bending, with better interpolating capabilities than its simpler counterpart is sought.

For the analysis of tube-like structures with macroelements, an ideal higher order element would exhibit quadratic variation of ϵ_y and γ_{xy} . Many trials were made to obtain an element based on a strain formulation with such features. 8, 9 and 10 DOF elements, some of them with rotational inplane degrees of freedom were investigated. However, the $\epsilon_x = 0$ assumption together with the compatibility requirement of Eq. (3.6) restricted the search somewhat.

A refined 6 node, 8 DOF strain based element with the same interpolating capabilities as the 9DOFD element was developed. This new element generally produces the same results as the 9DOFD element, but with one fewer DOF.

As stated earlier, a quadratic variation of ϵ_y is sought. Thus, consider the 6 node, 8 DOF element of Fig. 3.4 and the following strain field:
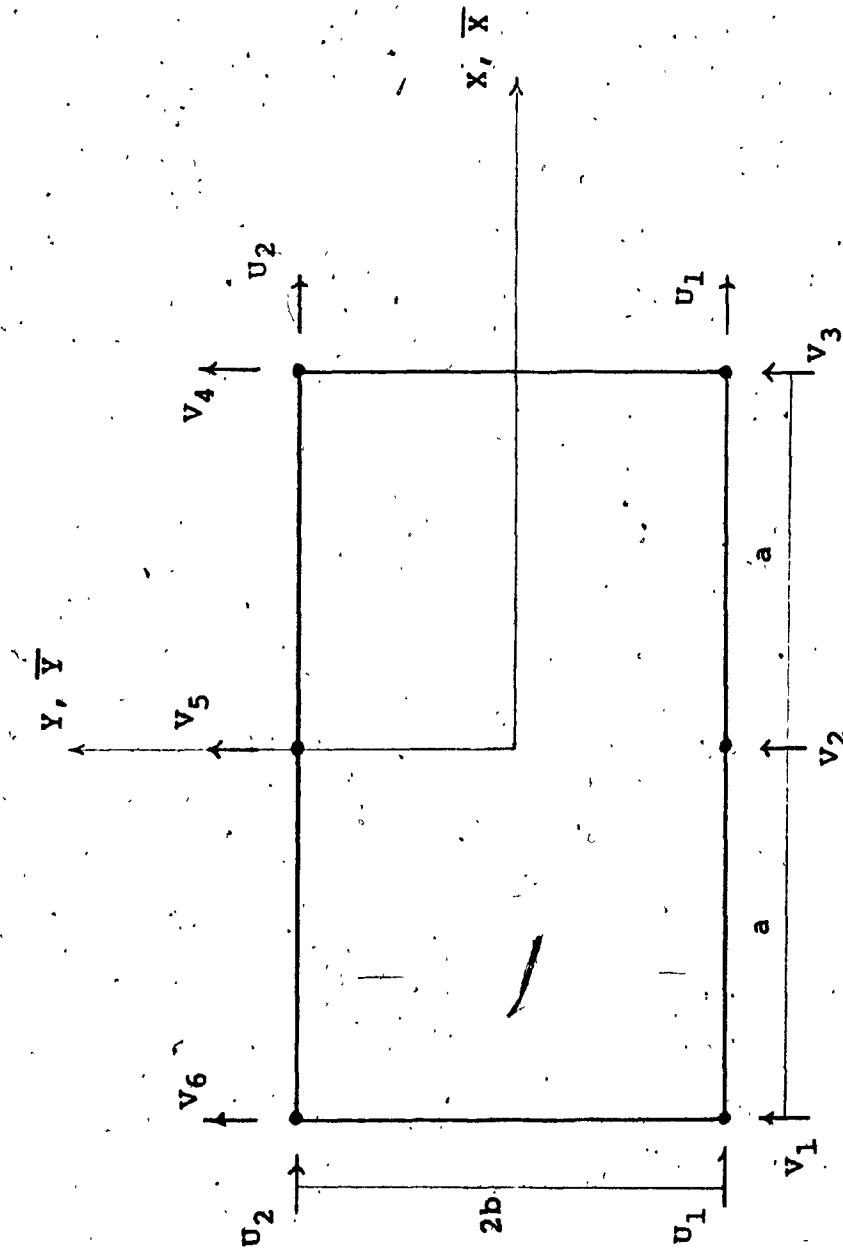
FIG. 3.4 – REFINED 8DOFS ELEMENT

$$\overline{X} = x/a \qquad \overline{Y} = Y/b$$

$$\begin{cases} \mathcal{E}_x = & 0 \\ \mathcal{E}_y = & A_4 + A_5 \ X + A_7 \ X^2 \\ \gamma_{xy} = & A_6 + 2A_7 \ XY + A_8 \ X \end{cases} \qquad (3.19)$$

Upon integrating the expressions for $\mathcal{E}_x$ and $\mathcal{E}_y$, the following displacement functions are obtained:

$$\begin{cases} U = C_1 \ (Y) \\ V = A_4 \ Y + A_5 \ XY + A_7 \ YX^2 + C_2 \ (X) \end{cases} \qquad (3.20)$$

where C_1 and C_2 are functions of Y and X respectively. The expression relating the shearing strain to the displacements U and V in Eqs. (3.3) yields:

$$\frac{dC_1}{dy} + \frac{dC_2}{dx} = -A_5 \ Y + A_6 + A_8 \ X \qquad (3.21)$$

Since C_1 is a function of Y only and C_2 of X only it follows that:

$$\begin{cases} C_1 = -A_5 \ Y^2 \ /2 + A_6 \ Y/2 \\ C_2 = A_8 \ X^2 \ /2 + A_6 \ X/2 \end{cases} \qquad (3.22)$$

Thus the displacement functions corresponding to the strain field as described by Eqs. (3.19) become:

$$\begin{cases} U = -A_5 \ Y^2 \ /2 \ + \ A_6 \ Y/2 \\ V = \ A_4 \ Y + A_5 \ XY + A_6 \ X/2 + A_7 \ YX^2 \ + A_8 \ X^2 \ /2 \end{cases} \qquad (3.23a)$$

These displacement functions are then added to those representing the rigid body motions Eqs. (3.4) to obtain the final displacement functions of the 8DOFS element:

$$\begin{cases} U = A_1 - A_3 \ Y - A_5 \ Y^2 \ /2 + A_6 \ Y/2 \\ V = A_2 + A_3 \ X + A_4 \ Y + A_5 \ XY + A_6 \ X/2 + A_7 \ XY^2 + \\ \quad A_8 \ X^2 \ /2 \end{cases} \qquad (3.23b)$$

The new displacement functions thus created render this element compatible for the V-degrees of freedom and incompatible in U (similar to 6DOFS). The transpose of the strain-displacement matrix is obtained as:

$$[B]^T = \begin{bmatrix} 0 & 0 & -1/2b \\ 0 & 0 & 1/2b \\ 0 & \overline{X}(1-\overline{X})/4b & (-1-2\overline{XY}+2\overline{X})/4a \\ 0 & (-1+\overline{X}^2)/2b & (\overline{XY}-\overline{X})/a \\ 0 & -\overline{X}(1+\overline{X})/4b & (1-2\overline{XY}+2\overline{X})/4a \\ 0 & \overline{X}(1+\overline{X})/4b & (1+2\overline{XY}+2\overline{X})/4a \\ 0 & (1-\overline{X}^2)/2b & (-\overline{XY}-\overline{X})/a \\ 0 & \overline{X}(-1+\overline{X})/4b & (-1+2\overline{XY}+2\overline{X})/4a \end{bmatrix} \qquad (3.24)$$

The corresponding 8x8 stiffness matrix is obtained as:

$$[K] = \begin{bmatrix} K1 & & & & & & & \\ -K1 & -K1 & & & & & & \\ K2 & -K2 & K3 & & & \text{SYMM.} & & \\ 0 & 0 & K4 & K9 & & & & \\ -K2 & K2 & K5 & K4 & K3 & & & \\ -K2 & K2 & K6 & K7 & K8 & K3 & & \\ 0 & 0 & K7 & K10 & K7 & K4 & K9 & \\ K2 & -K2 & K8 & K7 & K6 & K5 & K4 & K3 \end{bmatrix}$$

in which:

$$K1 = Gtr \qquad\qquad (3.25)$$

$$K2 = Gt/2$$

$$K3 = 2Ert/15 + 25Gt/36r$$

$$K4 = Ert/15 - 8Gt/9r$$

$$K5 = -Ert/30 + 7Gt/36r$$

$$K6 = Ert/30 - Gt/36r$$

$$K7 = -Ert/15 - 4Gt/9r$$

$$K8 = -2Ert/15 + 17Gt/36r$$

$$K9 = 8Ert/15 + 16Gt/9r$$

$$K10 = -8Ert/15 + 8Gt/9r$$

3.3.3- COMPARISON OF FORMULATIONS

Once again one may observe that the strain based element's displacement functions are coupled while those of the displacement based 9DOFD element are independent of each other.

The main feature about these two refined elements, in

- 51 -

contrast with the simple ones, is that <u>both</u> are able to describe linear direct strain and an independent constant shearing strain. Both elements can also deform in the proper shape, i.e., with curved edges (Fig. 3.2a)), when subjected to pure bending. Thus, they are both expected to perform well in a bending mode.

3.4- <u>EVALUATION OF ELEMENT PERFORMANCE</u>

A cantilever beam subjected to transverse loading is chosen as a test problem due to its similarity to a tall building system subjected to lateral loading. The main objective is to examine the comparative performance of the four elements presented in the previous sections.

Three test problems are carried out on the cantilever beam. The first problem looks at the performance of each of the four elements when analysing a cantilever beam with various aspect ratios subjected to a concentrated load at its free end. By varying the aspect ratio, one can study element performance for various degrees of shear to bending deformation ratios. The second problem examines two other loading arrangements and the third the rate of convergence of the various elements.

The maximum vertical deflection and the maximum normal stress of the cantilever obtained by the displacement and strain based elements are compared to theory of elasticity and engineering beam theory solutions.

- 52 -

3.4.1- EX.3.1 (CANTILEVER BEAM WITH VARIOUS ASPECT RATIOS)

The first test consists in analysing a cantilever beam with various aspect ratios subjected to a concentrated load at its free end (Fig. 3.5). The beam is divided into 16 elements. The beam aspect ratio, AR, defined as the ratio of total length over beam depth, is varied accordingly: AR = 2.5, 4, 10 and 20, representing a deep, moderately deep, slender and very slender beam, respectively.

The significance of varying the aspect ratio is to test a cantilever beam with different degrees of shear to bending deformation ratios. For the deep beam, bending deformations account for 87 % of total deflection, 94 % for the moderately deep beam and 99.1 % & 99.8 % for the slender and very slender beams respectively.

The aspect ratio is modified by varying the depth while keeping the other dimensions constant. The results for maximum deflection at the free end using both simple and refined elements are presented in Table 3.1.

The 'exact' values for maximum deflection in Table 3.1 for the deep and moderately deep beams are theory of elasticity solutions while engineering beam theory was deemed sufficient for the slender and very slender beams (less than 0.2 % error). A figure in parentheses in Table 3.1 represents the percentage error in maximum deflection for a given element.
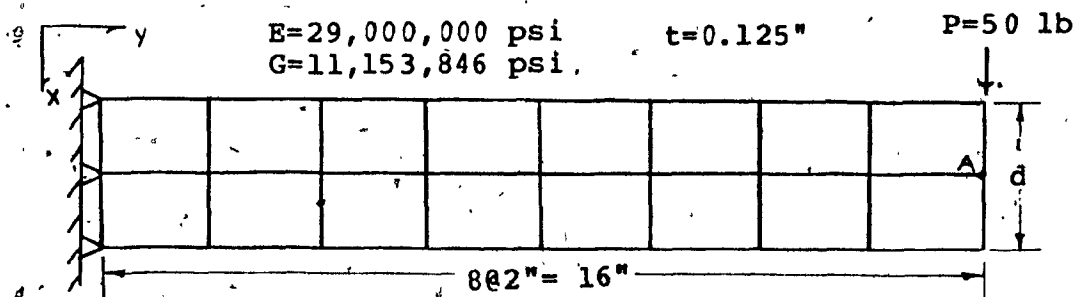
FIG. 3.5 - CANTILEVER BEAM SUBJECTED TO POINT LOAD

1"=25.4 mm
1 psi = 6.8948 kPa
1 lb = 4.4482 N

		DEEP	MODER. DEEP	SLENDER	VERY SLENDER
BEAM AR		2:5	4	10	20
D_A - EXACT		.000997	.00375	.05560	.4422
SIMPLE ELEMENTS	6DOFD	.000917(-8.0%)	.00335(-10.7%)	.03469(-37.6%)	.1299 (-70.6%)
	6DOFS	.000948(-4.9%)	.00366(-2.4%)	.05532(-9.5%)	.4404 (-0.4%)
REFINED ELEMENTS	9DOFD	.000964(-3.3%)	.00369(-1.6%)	.05538(-0.4%)	.4405 (-0.4%)
	8DOFS	.000964(-3.3%)	.00369(-1.6%)	.05538(-0.4%)	.4405 (-0.4%)

TABLE 3.1 - MAXIMUM DEFLECTION AT A FOR VARIOUS ELEMENTS (in.)

The results indicate that not only does the strain based simple 6DOFS element perform well when bending is predominant (AR = 10,20) but also performs better than the displacement based 6DOFD element when shear deformations are of greater importance (AR = 2.5,4). When bending is predominant (99.1 and 99.8 % of total deflection), the 6DOFS element is the only simple element that gives satisfactory results.

Both refined elements perform well when they are subjected to various degrees of shear to bending deformation ratios. The strain based 8DOFS element produces the same results as the displacement based 9DOFD element but with one fewer degree of freedom.

3.4.2- **EX.3.2 (CANTILEVER BEAM SUBJECTED TO PURE BENDING AND UNIFORM LOAD)**

The slender cantilever beam is now loaded for two new cases: a uniformly distributed load and an applied moment. Keeping in mind our goal of analysing tall building systems, these two new loading cases represent other possible lateral load systems to which a tall building is subjected to. This test problem is also to verify whether the strain based 6DOFS element performs as well under other loading arrangements.

The slender beam is modelled with 16 elements as in the previous example and the results for maximum vertical

- 55 -
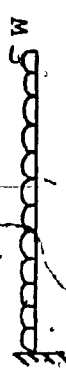
TYPE OF LOADING

		P=50 lb (222.4 N)	W=.625 lb/in (109.5 N/M)	M=80 ... in (9.04 N-M)
	BEAM THEORY	$\dfrac{PL^3}{3EI} + \dfrac{6PL}{5GA} = .05569$	$\dfrac{WL^4}{8EI} + \dfrac{3WL^2}{4GA_r} = .04203$	$\dfrac{ML^2}{2EI} = .008276$
SIMPLE ELEMENTS	6DOFD	.03469 (-37.6 %)	.002631 (-37.4 %)	.005169 (-37.5 %)
	6DOFS	.05532 (-0.5 %)	.004190 (-0.3 %)	.008276 (0.0 %)
REFINED ELEMENTS	9DOFD	.05538 (-0.4 %)	.004196 (-0.2 %)	.008283 (+0.1 %)
	8DOFS	.05538 (-0.4 %)	.004196 (-0.2 %)	.008283 (+0.1 %)

TABLE 3.2 — MAXIMUM DEFLECTION AT FREE END FOR VARIOUS LOADING CASES

deflection are given in Table 3.2.

It is observed that the percentage error in the maximum deflections obtained for various loading cases vary little. For all three loading conditions, the simple displacement based 6DOFD element gives approximatively 38 % error in the maximum deflection, while the strain based 6DOFS element produces results all within 1 % of the engineering beam theory results. This is a significant achievement for an element possessing the same number of degrees of freedom.

Once again, the refined elements both produce good results. The strain based 8DOFS element, with one fewer degree of freedom than the displacement based 9DOFD element gives identical results.

3.4.3- EX. 3.3 (CONVERGENCE TEST)

A convergence test will now be performed for the analysis of a slender cantilever beam where bending is predominant. The dimensions, loading arrangements and convergence curves are presented in Figs. 3.6, 3.7 and 3.8. The meshes used in the convergence study consisted in: 1x10, 2x20, 3x30 (square elements) and 1x5, 2x10, 3x15 & 4x20 (rectangular 2:1 elements).

Fig. 3.6 gives the maximum deflection as obtained by the simple elements. The two lower curves are those of the displacement based 6DOFD element and the two higher curves, those of the strain based 6DOFS element.
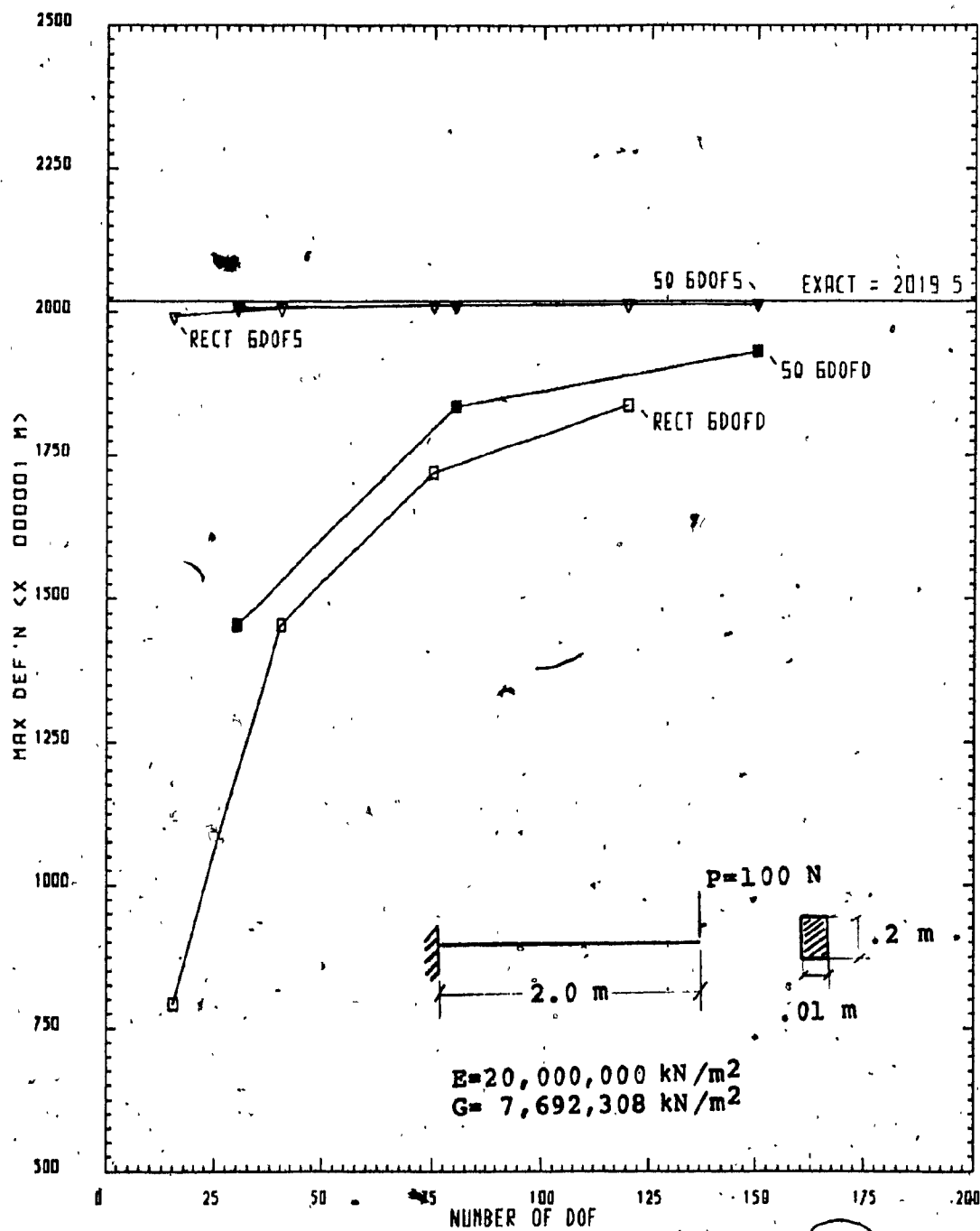
FIG. 3.6 – CONVERGENCE FOR Dmax (SIMPLE ELEMENTS)
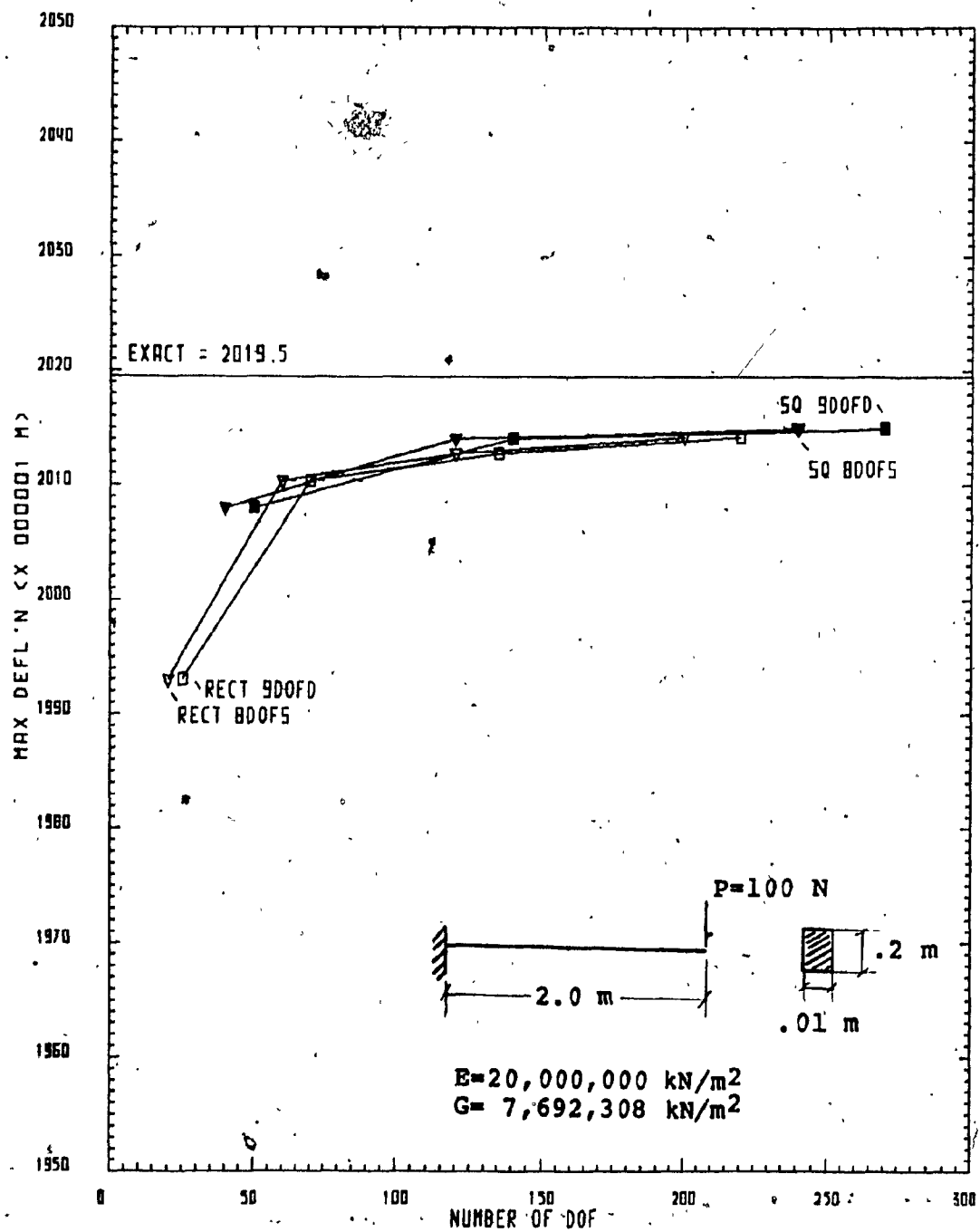
FIG. 3.7 — CONVERGENCE FOR Dmax (REFINED ELEMENTS)
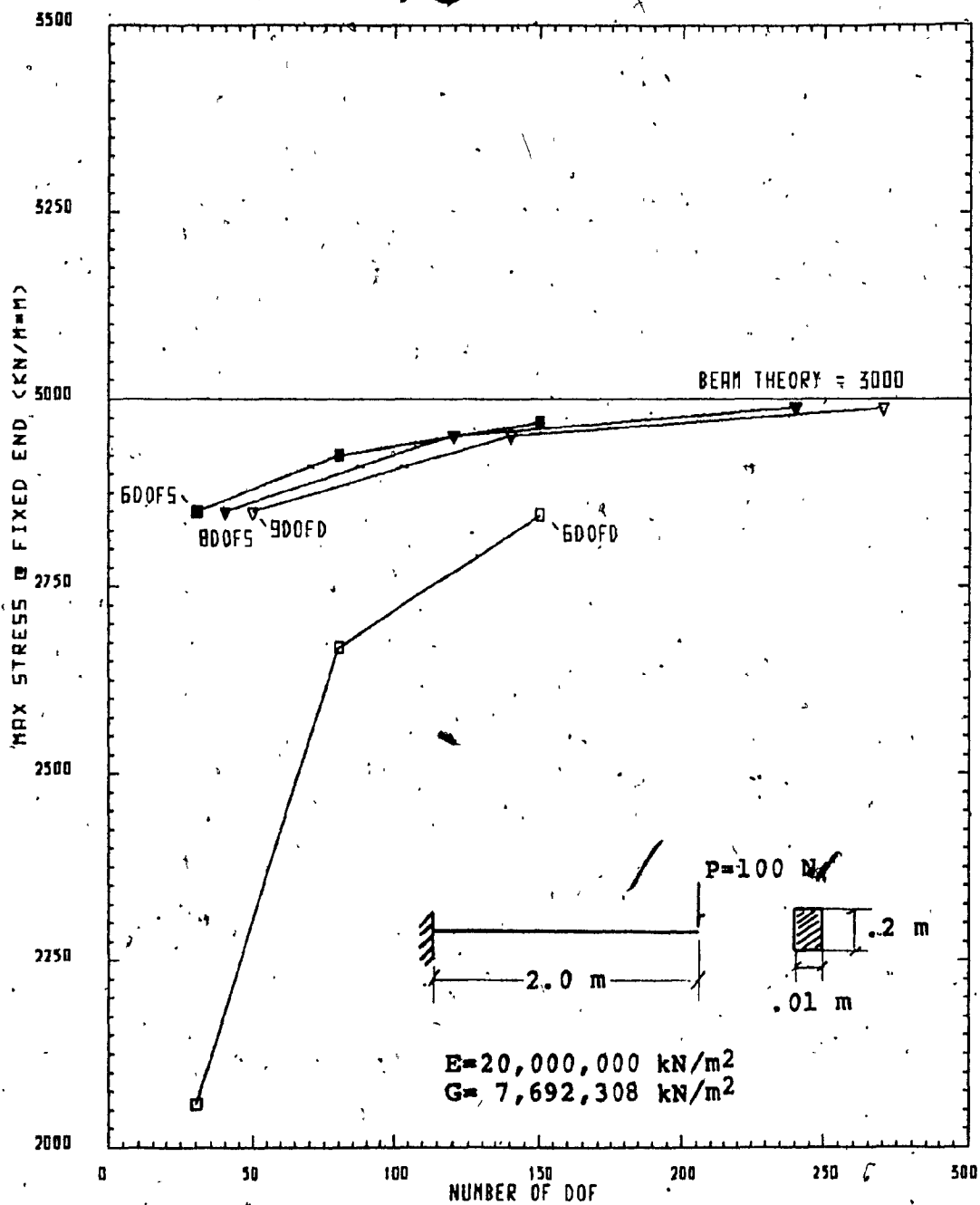
FIG. 3.8 – CONVERGENCE FOR MAXIMUM STRESS

The strain based 6DOFS element shows a very fast convergence rate. For example: 10 6DOFS elements produce a Dmax = 20.08 (99.4 % of exact) while 10 6DOFD elements produce a Dmax = 14.54 (72.0 % of exact).

Square elements based on an assumed displacement field behave better than their rectangular counterparts, while the performance of the 6DOFS element does not seem to be affected by its shape.

The maximum deflections obtained with the refined elements converge rapidly for this particular test problem and are slightly affected by the element aspect ratio (Fig. 3.7). Note that both the horizontal and vertical scales of Fig. 3.7 are not the same as those of Fig. 3.6.

Generally, for a given number of elements, the 9DOFD and 8DOFS elements produce the same results. Due to one less degree of freedom in the strain based refined element, a slightly higher convergence rate is attained.

Results for the maximum normal stress at the fixed end of the cantilever beam produce the same basic convergence pattern (Fig. 3.8). The refinement however, from a 6 DOF element to a higher order refined element does not significantly improve the convergence rate.

3.4.4 - SUMMARY OF RESULTS

The performance of the simple elements can be summarized as follows:

1- The strain based 6DOFS element performs remarkably well in simulating both shear and bending behaviour.

2- As the amount of bending is gradually increased, the performance of the displacement based 6DOFD element deteriorates.

3- The aspect ratio of the 6DOFS element does not seem to influence its behaviour (i.e., a mesh of square and of rectangular elements produce similar convergence properties and accuracy).

4- The 6DOFS element demonstrates a much faster convergence rate than the 6DOFD element.

The performance of the refined elements can be summarized as follows:

1- Both the 8DOFS and 9DOFD elements perform well in a predominantly bending deformation mode.

2- The refined elements seem to be little affected by their aspect ratios.

3- The difference in results between the two elements is insignificant.

4- The strain based 8DOFS element has a slightly faster

convergence rate than the displacement based 9DOFD
element.

CHAPTER IV

NUMERICAL EXAMPLES OF
MACROELEMENT ANALYSIS

4.1- INTRODUCTION

In this chapter several numerical examples on the macroelement technique using the new strain based elements are presented. A modified version of Moselhi's TUBE program [21] is used to test the performance of these elements in both static and dynamic analyses.

Even though the program TUBE was developed for the analysis of framed-tube, three dimensional structures, it is used here for the analysis of planar wall-frames. The analysis of planar frames permit the results to be compared to those obtained with other plane frame analysis packages.

The objective of the testing is to investigate the behaviour of the strain based elements when applied to the macroelement technique. More precisely, testing should first verify whether the strain based elements are capable of reconstituting the overall lateral stiffness to produce realistic values for the maximum lateral deflection and natural frequency. Secondly, the interpolating capabilities of the strain based elements for producing a good approximation of the internal member forces is examined.

Four numerical examples are considered. The first two

examples are concerned with the static and dynamic analyses of tall planar frames. In these examples, the effects of mesh size and the choice of element on the maximum lateral deflection, natural frequency and internal member forces are investigated. The third and fourth examples examine the capability of the strain based elements in analysing tall core structures where bending behaviour is predominant.

4.2- <u>STATIC ANALYSIS OF A TALL PLANAR FRAME</u>

Consider the 40 storey, 14 bay planar frame of Fig. 4.1, subjected to a uniformly distributed lateral loading. The dimensions of the members and joints are somewhat typical of those found in the facade of a framed tube.

The results from TUBE will be compared to those of TABS [27]. TABS is a computer program for the linear analysis of frame and shear wall buildings subjected to both static and dynamic loadings. TABS treats the floors as rigid diaphragms allocating one lateral translational degree of freedom per floor together with one vertical and one in-plane rotational degree of freedom per joint. Despite its inability for taking advantage of the structure symmetry conditions, TABS is a relatively efficient program.

With TABS, bending and shear deformations are considered in all members. To evaluate the effects of the
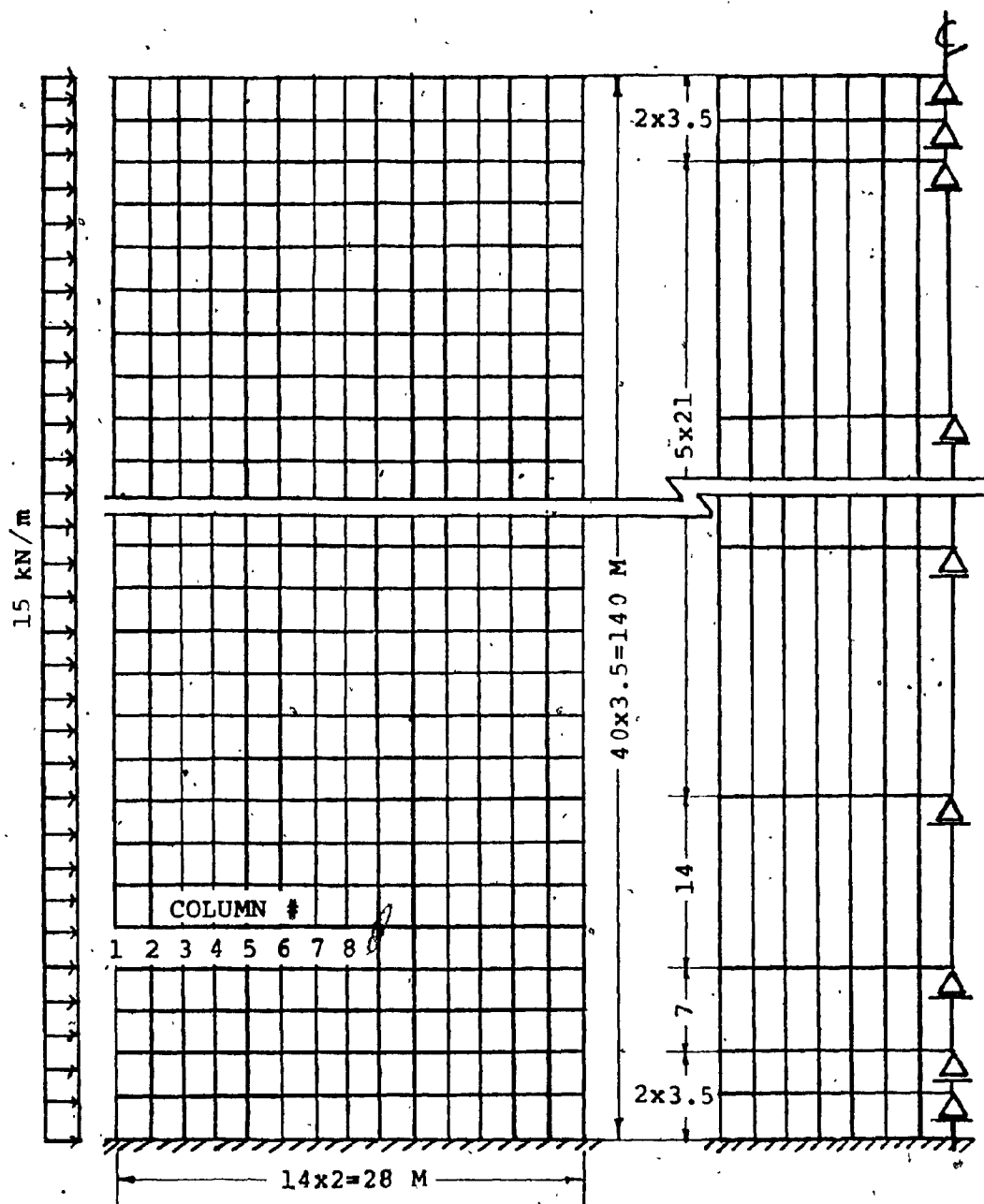
a) ELEVATION

b) MODEL - MESH 1

E=20,685,000 kN/m^2
G= 8,618,750 kN/m^2

c) STRUCTURE PROPERTIES

TYP. COL.
0.6x0.6 m

TYP. BEAM
1.0x0.3 m

FIG. 4.1 - 40 STOREY, 14 BAY PLANAR FRAME

finite size joints two analyses are performed. The first uses centerline dimensioning, TABS CL (finite size joints ignored) while the second, TABS RA, uses rigid arms to simulate the finite size of the joints. The 'CL' or 'RA' attachment to TABS is simply a notation used to designate the centerline and rigid-arm analyses. TABS CL and TABS RA provide upper and lower bounds of the overall lateral stiffness respectively, because the actual joints do experience some deformations.

4.2.1- STRUCTURE IDEALIZATION

. With the TUBE program, only half the structure need be analysed due to symmetry conditions. The equivalent elastic properties of the membrane were found to be:

E = 12,327,190 kN/m^2

G = 507,479 kN/m^2

The equivalent structure is then discretized using 70 macroelements labelled as Mesh 1, Fig. 4.1b). The number of degrees of freedom (DOF) used with Mesh 1 varies according to which element is used. Both simple elements, 6DOFD and 6DOFS, use 80 DOF of which only 20 DOF are retained for the final structure stiffness matrix. With the refined elements, 20 DOF are retained from 150 and 160 DOF using the 8DOFS and 9DOFD elements, respectively.

TABS retains 40 DOF from a total of 1240 degrees of

freedom, a very significant difference in computational effort as indicated by the execution times of the various analyses given in Table 4.1.

4.2.2- MAXIMUM LATERAL DEFLECTION

Results for the maximum lateral deflection, axial and shear forces at mid-height of the corner column of the 5-th storey are given in Table 4.1. The execution time of each run is given in the last row of the Table.

| | TABS | | TUBE | |
	Center-line	Rigid arms	SIMPLE 6DOFD/6DOFS	REFINED 9DOFD/8DOFS
Dmax,m	.161	.093	.145/.147	.147/.147
P, Kn	1634	1563	1656/1681	1672/1677
V, Kn	51	40	57/34	-3/-3
CP Sec exec. time	58.3	58.0	5.8/5.8	8.6/8.2

TABLE 4.1. Dmax, P & V OF CORNER COLUMN ON 5-th FLOOR OF 40 STOREY, 14 BAY PLANAR FRAME.

With TABS, the modelling of the joints with rigid arms overestimates the overall lateral stiffness due to the actual flexibility within the joint. This results in a lower bound value for the maximum lateral deflection, Dmax. The modelling using centerline dimensioning on the other

hand, underestimates the overall lateral stiffness by completely ignoring any stiffness provided by the joints and thus yields a higher bound value for Dmax. As the macroelement technique can account for the deformability of the finite sized joint, the maximum lateral deflection obtained with TUBE is expected to fall in between the upper and lower bound values of TABS and this is the case as can be seen in Table 4.1.

The maximum lateral deflection is little affected by the choice of element. This is somewhat surprising after the conclusions on element performances in the last chapter where the displacement based 6DOFD element was found to be too stiff. As indicated in Table 4.1, the 6DOFD element produces a maximum lateral deflection of similar magnitude to that obtained with the other elements.

This is explained by the second conclusion made on the simple elements in Chapter III. It stated, that as the amount of bending is increased, the performance of the displacement based 6DOFD element deteriorates. In this 40 storey, 14 bay frame, the shear deformation mode is still very significant and both simple elements behave in a similar manner.

The shear to bending deformation ratio is not only a function of a building's aspect ratio but also of the stiffness parameters E and G. In this example, the ratio E/G is approximatively 24/1, thus suggesting a significant shear deformation mode.

In a solid section, such as the cantilever beams tested in Chapter III where the strain based 6DOFS element proved to be a better simple element, this ratio was 2.6/1. This indicates that the simple strain based 6DOFS element would behave better than its displacement based counterpart only in the analysis of shearwalls and corewalls where bending deformations are more important. This will be verified in later sections.

4.2.3- INTERNAL MEMBER FORCES

The internal member forces as obtained with the macroelement technique are of a very approximative nature. This is dramatically illustrated by examining the outer column shear force in Table 4.1.

At first sight, it seems that the shear forces obtained by the simpler elements are more accurate than those by the refined elements. This anomaly can be explained as follows.

At the edge of the continuum membrane, or for that matter of the frame members, the shear stress is non-existent as exhibited by the results of the refined elements. Since in the simple elements, the shear stress distribution is constant in the direction of the building depth, some shear stresses seem to appear at the edge. A similar situation is created if a coarser mesh is used with the refined elements as will be seen in the next section.

However in the real frame, which is not a continuum, despite of its zero shear stress on a member edge, the resultant shear force in the member is not zero. Thus Eq. (2.12) which relates the column shear stress directly to the membrane shearing stress is definitely in error. The inadequacies of the method used in the macroelement technique for determining the internal member forces will be discussed further in Chapter V.

4.2.4- EFFECT OF MESH SIZE

	TABS		TUBE	
	Center-line	Rigid-arms	SIMPLE 6DOFD/6DOFS	REFINED 9DOFD/8DOFS
Mesh 1	.161	.093	.145/.147	.147/.147
Mesh 2	.161	.	.143/.146	.147/.147
Mesh 3	.161	.09	.139/.145	.147/.147

TABLE 4.2. MAXIMUM LATERAL DEFLECTION (m) OF 40 STOREY, 14 BAY PLANAR FRAME FOR VARIOUS MESHES.

In order to investigate the particular behaviour of each element, two other meshes, using 21 macroelements with 14 degrees of freedom retained for the structure stiffness matrix and 10 macroelements with 10 DOF retained, are considered. As shown in Figs. 4.1 and 4.2, Mesh 1 is the finest and Mesh 3 the coarsest. Note that the mesh is

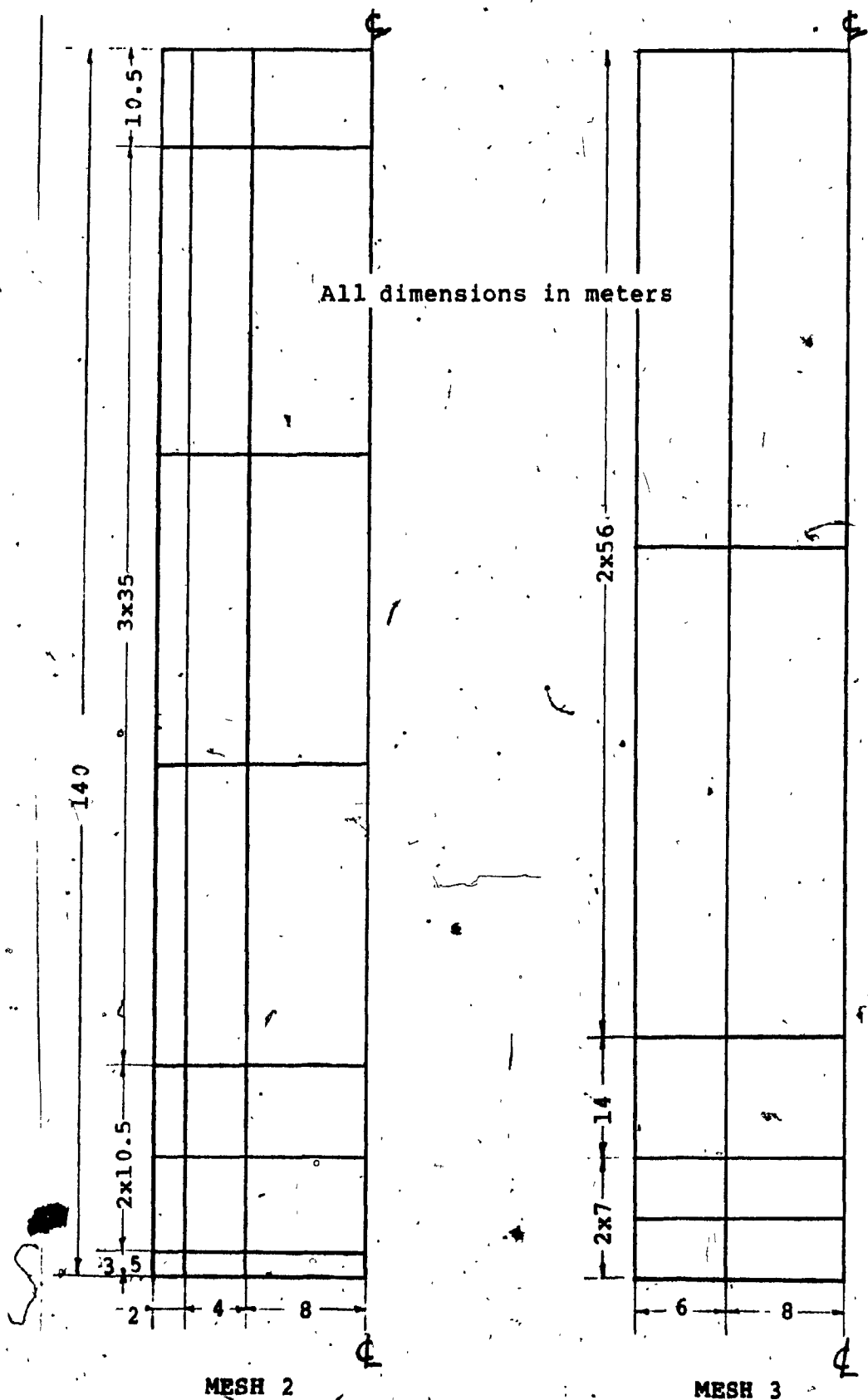All dimensions in meters

MESH 2

MESH 3

FIG. 4.2 - MESHES 2 & 3 FOR 40 STOREY, 14 BAY PLANAR FRAME

kept fine along the outer edge and lower floors. This is to better approximate the sharp gradient in the axial force distribution at these locations. The variation of column axial and shear forces at mid-height of the 5-th storey for all three meshes are given in Figs. 4.3 to 4.8. These figures illustrate how the internal member forces are affected by element choice.

In Table 4.2, we notice that the maximum lateral deflection is not affected by mesh size when the refined elements are used. With the simple elements, Dmax varies only slightly. All four elements give comparable results with the simple displacement based 6DOFD element being most affected by the mesh selection.

The results from TABS indicate a moderate degree of shear lag, as can be seen by the non-linearity of the axial force distribution along the building's depth (Fig. 4.3). This shear-lag is expressed as an increasing slope in the axial force distribution as one goes from the inner to the outer columns.

It is interesting to note that all four elements produce a decreasing outward slope in the axial force distribution, Fig. 4.3. This can be attributed to the stiffer edges of the continuum caused by the assumption of a grid unit bounded by four inflection points used in deriving the equivalent elastic properties. While the complete grid unit may be representative of the major portion of a planar frame, it is certainly not valid along the boundaries. In
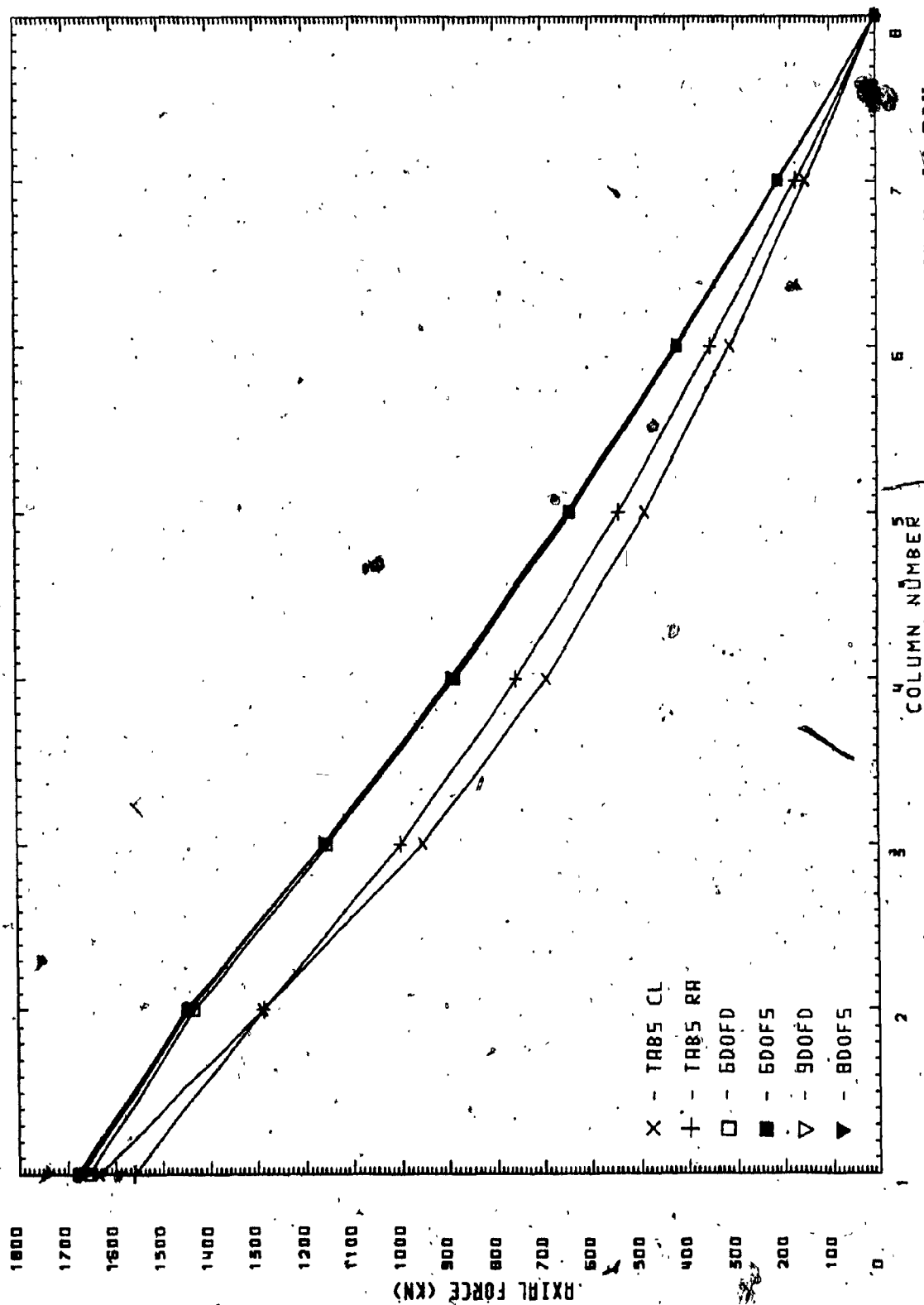
FIG. 4.2 - VARIATION OF AXIAL FORCES AT 5-th FLOOR OF 40 STOREY, 14 BAY
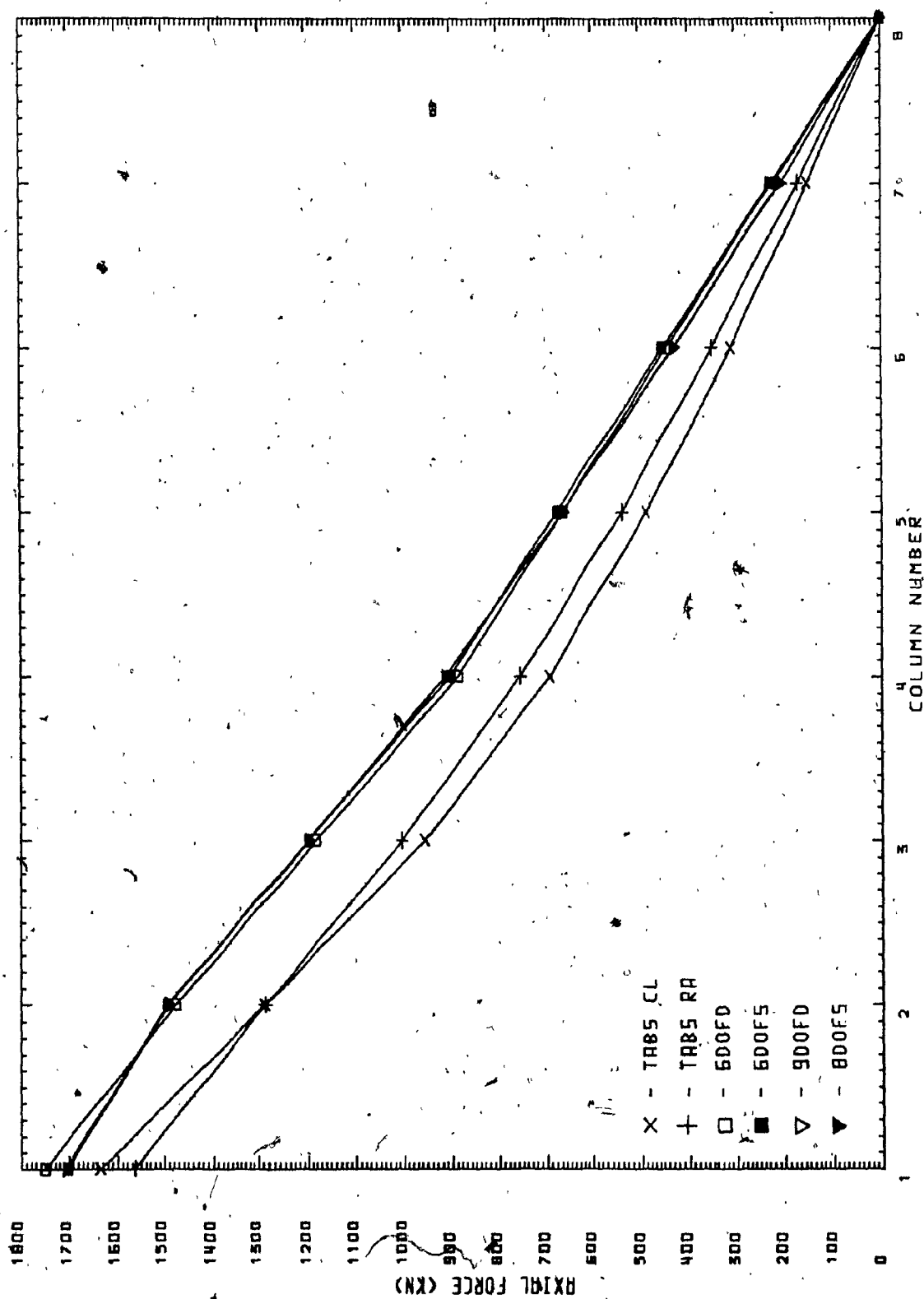PLANAR FRAME - MESH 1

FIG. 4.4 - VARIATION OF AXIAL FORCES AT 5-th FLOOR OF 40 STOREY, 14 BAY
PLANAR FRAME - MESH 2
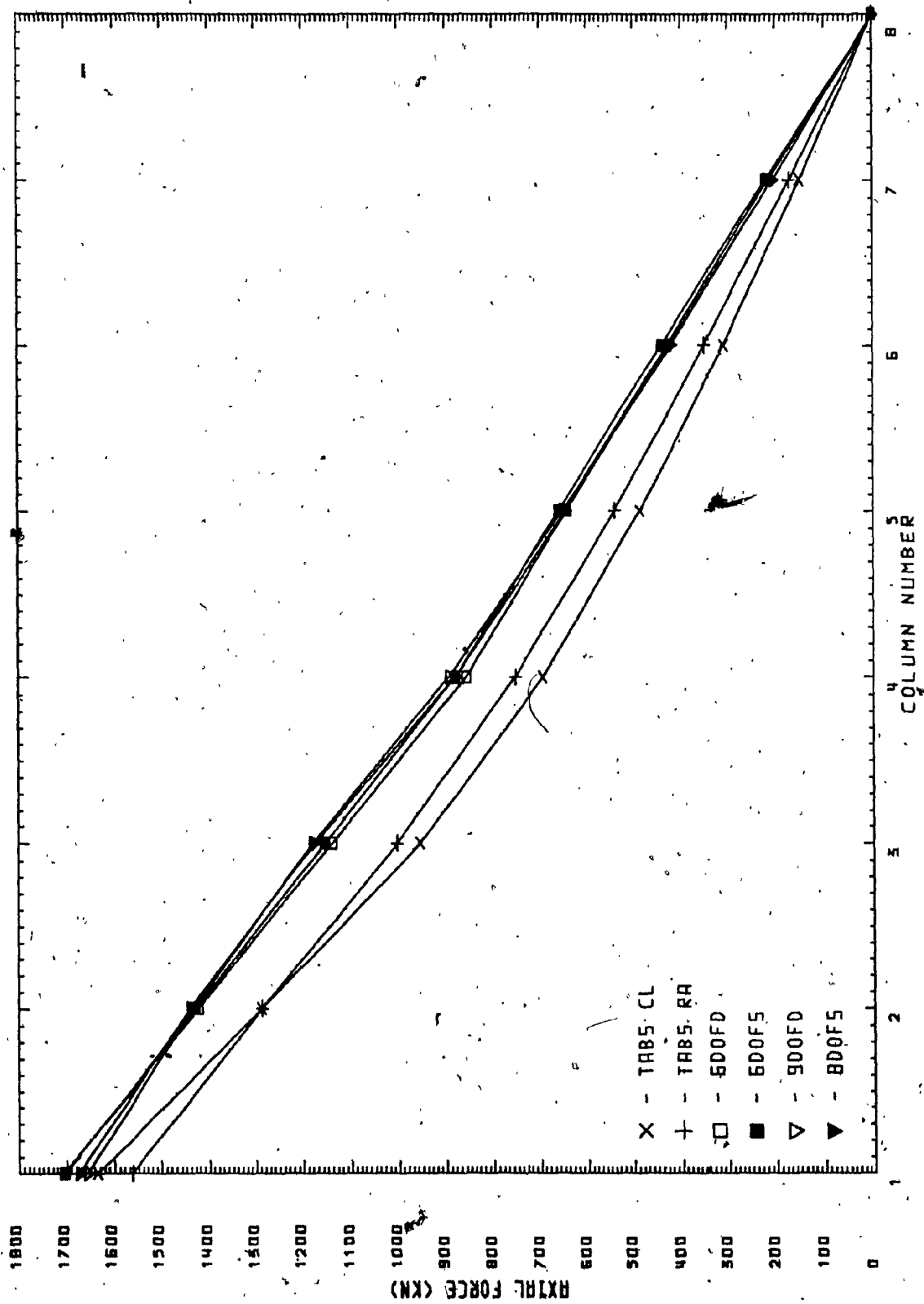
FIG . 4.5 - VARIATION OF AXIAL FORCES AT 5-th FLOOR OF 40 STOREY, 14 BAY
PLANAR FRAME - MESH 3

fact, along the boundaries, a half grid unit would be more appropriate.

The complete grid assumption, therefore, causes an overestimation of the equivalent elastic properties along the membrane edges. This overestimation in turn, produces lower stresses along the boundary of the continuum.

The most obvious effect of varying the mesh size on element performance is the distribution of internal member forces. For example, in Fig. 4.5, (Mesh 3), where the outer element spans over the first four columns, the simple elements produce a linear distribution while the refined elements produce a quadratic variation of axial forces in the columns.

The shear force distribution is more affected by mesh size (Figs. 4.6 to 4.8). This is demonstrated by observing that the simple and refined elements produce constant and linear shear force distributions respectively.

Note once again, the inadequate approximation of the outer column shear force exemplified by the refined elements in Mesh 1. Even though the simple elements provide a good approximation to the actual shearing stress, the refined elements with their linear interpolation, can better represent the parabolic distribution.

Another interesting observation is that the 8DOFS element, with one fewer degree of freedom, produces very similar results to the 9DOFD element.
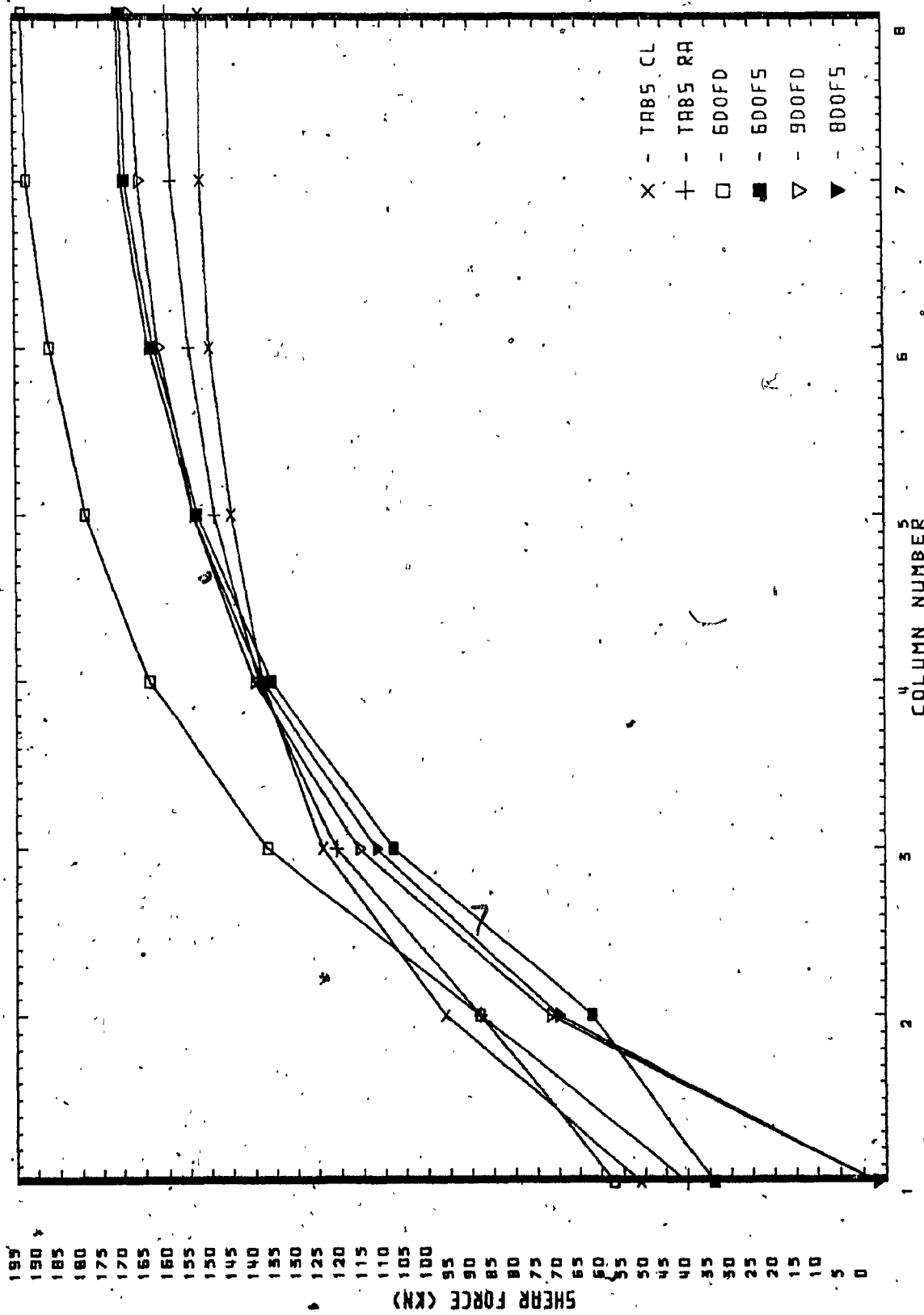
FIG. 4.6 – VARIATION OF COLUMN SHEAR FORCES AT 5-th FLOOR OF 40 STOREY, 14 BAY
PLANAR FRAME – MESH 1
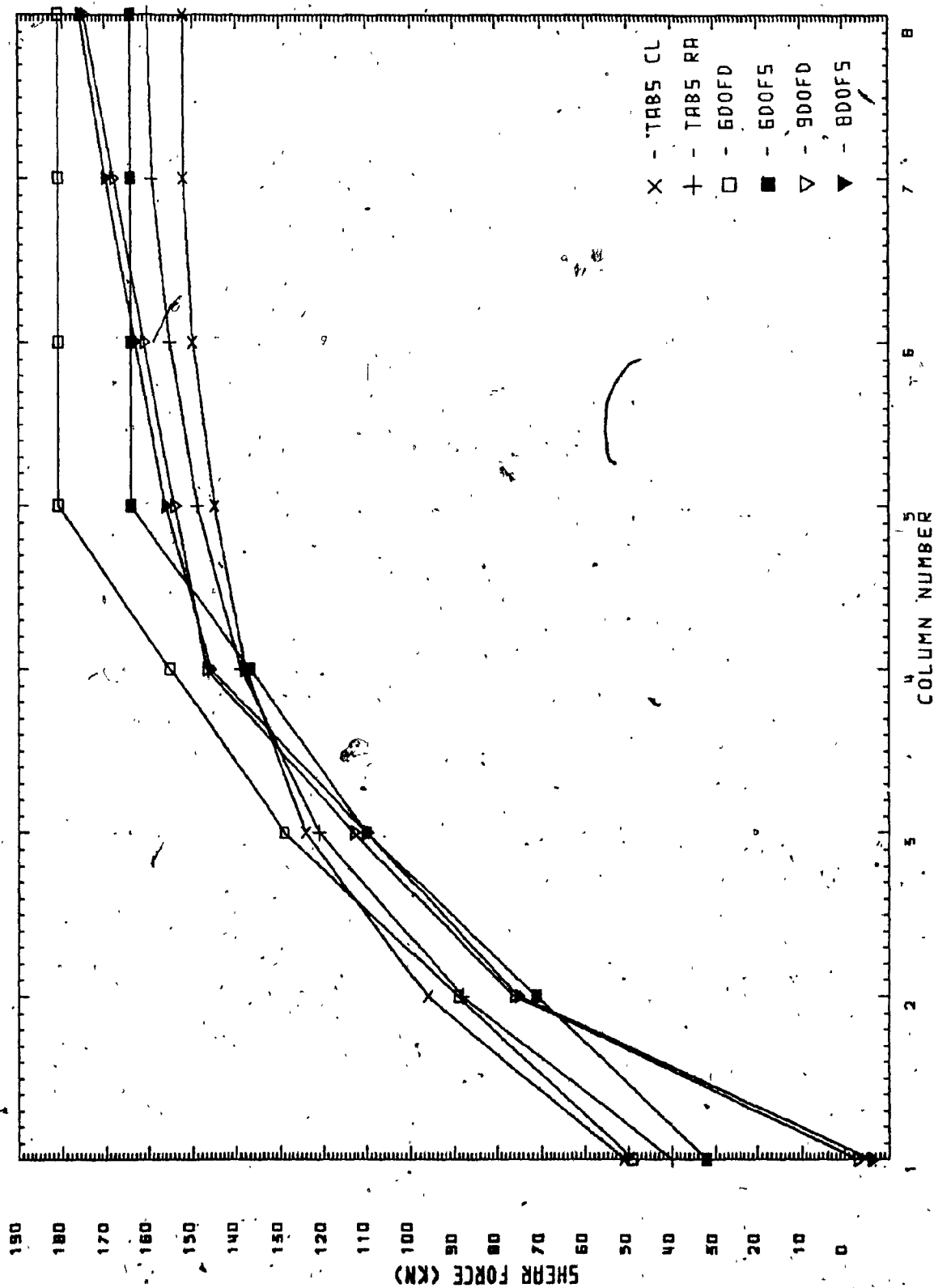
FIG. 4.7 - VARIATION OF COLUMN SHEAR FORCES AT 5-th FLOOR OF 40 STOREY, 14 BAY PLANAR FRAME - MESH 2
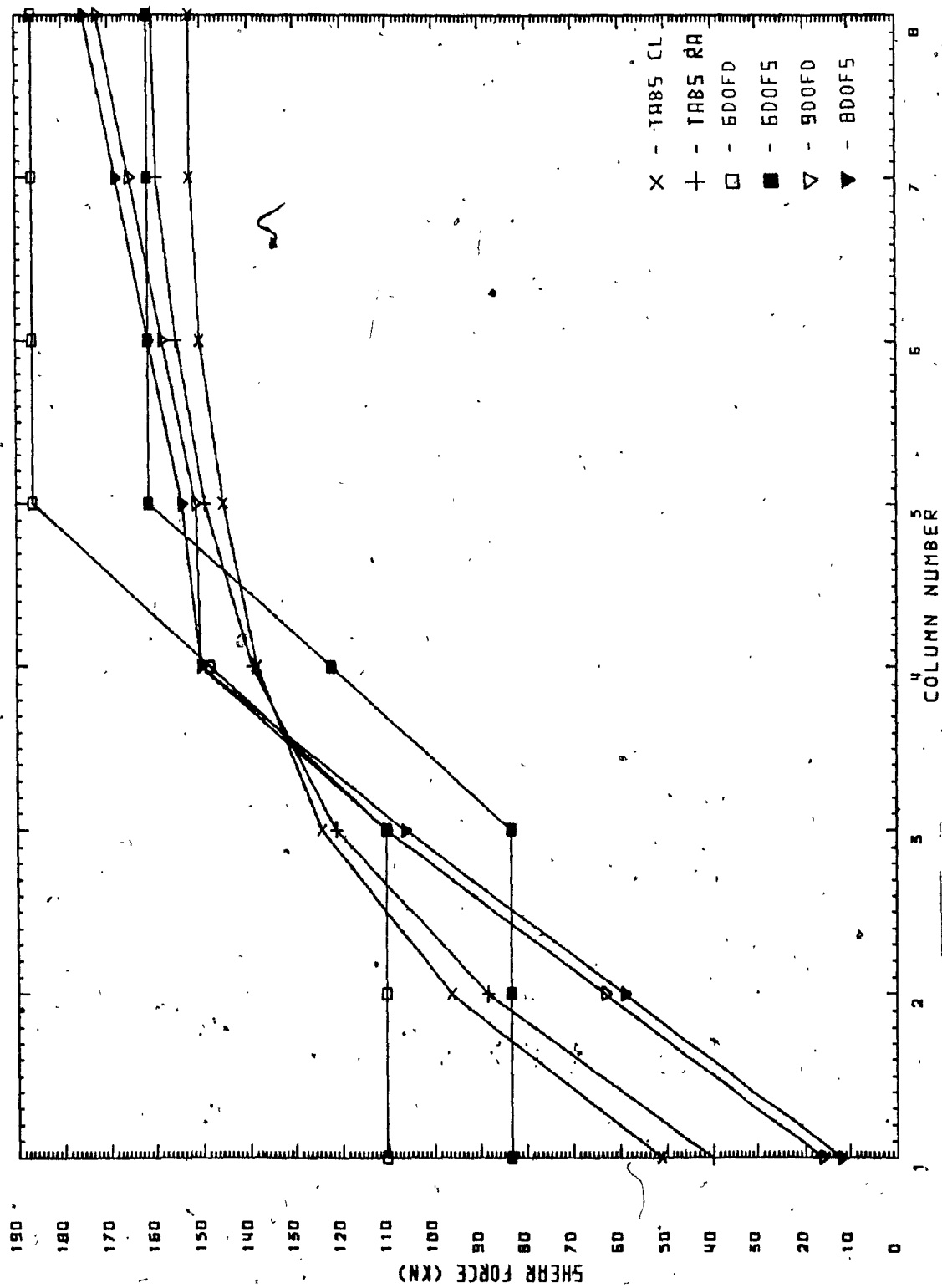
FIG. 4.8 — VARIATION OF COLUMN SHEAR FORCES AT 5-th FLOOR OF 40 STOREY, 14 BAY
PLANAR FRAME — MESH 3

4.3- DYNAMIC ANALYSIS OF A TALL PLANAR FRAME

Consider the 40 storey, 16 bay planar frame of Fig. 4.9 analysed by Mule [23] for natural frequencies with the refined 9DOFD element. The structure has the following properties along with those given in Fig. 4.9:

    Storey height = 12' (3.66 m)
    Lumped weight per storey = 1800 kips (8007 kN)
    E = 3 000 000 psi (20 684 400 kPa)
    G = 1 250 000 psi (8 618 500 kPa)

Mule selected to use the refined element over the simple displacement based element because he had found that the 6DOFD element was too stiff in bending and produced inaccurate results when used in very tall building analysis.

This 40 storey, 16 bay planar frame has an aspect ratio equal to four and therefore, in a building context, can be considered as a tall slender structure. All four elements, simple and refined, will be used for determining the natural frequencies of this planar frame.

The natural frequencies obtained with TUBE are compared to those obtained by TABS [27]. As in the previous example, two analyses are performed with the TABS program. The first ignores the finite size of the joints and uses centerline dimensioning. Since the actual joints do contribute to the lateral stiffness, the overall lateral stiffness is
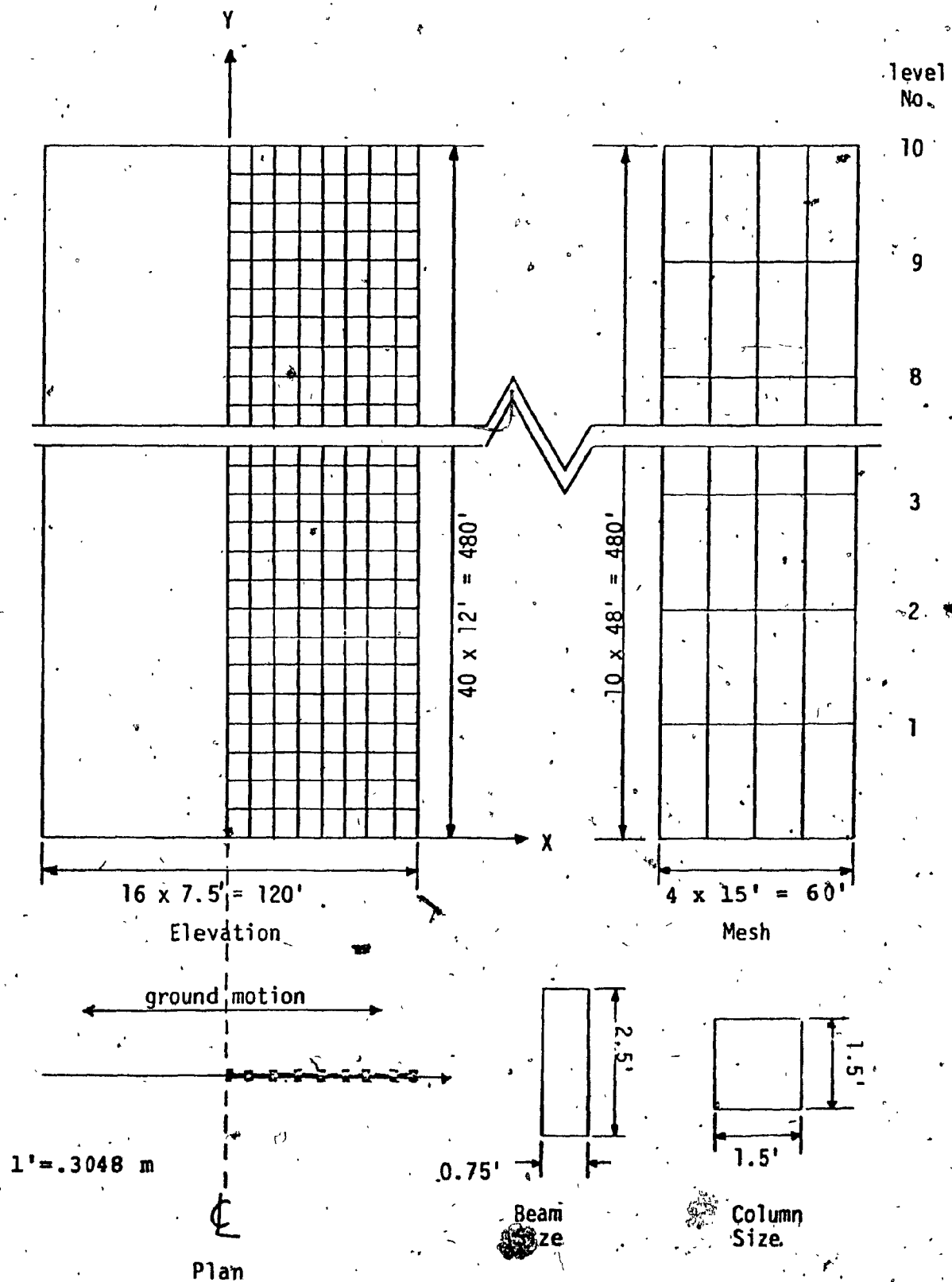
FIG. 4.9 - 40 STOREY, 16 BAY PLANAR FRAME, [23]

underestimated thus producing a lower bound value for the natural frequencies. The second TABS analysis treats the finite sized joints as completely rigid thus overestimating the lateral stiffness and providing a higher bound value for the natural frequencies.

Both shear and bending deformations are considered in all members with TABS. The mass is lumped at each floor level and 40 degrees of freedom are retained as the global degrees of freedom from a total of 1400 DOF.

With TUBE, only half the structure need be analysed for reasons of symmetry. The structure is replaced by an equivalent orthotropic membrane which is subsequently divided into equal size macroelements for ease of data preparation. The elastic properties of the equivalent membrane are determined as :

$$\overline{E} = 171\ 885\ 036\ psf\ (8\ 229\ 856\ kPa)$$
$$\overline{G} =\quad 3\ 120\ 752\ psf\ (\quad 149\ 422\ kPa)$$

With TUBE the mass is lumped on 10 levels. Note that the coarser mass distribution than that used in the TABS analyses is probably the biggest source of approximation in this technique. The TUBE program retains 10 translational degrees of freedom for the global structure stiffness matrix for natural frequency calculations. Initially the simple elements modelled the structure using 50 DOF, the 8DOFS element used 90 DOF and the 9DOFD element used 100 DOF.

Table 4.3 gives the first four natural frequencies.

	TABS		TUBE	
Freq.	Center-line	Rigid arms	SIMPLE 6DOFD/6DOFS	REFINED 9DOFD/8DOFS
W1	.530	.686	.590/.589	.587/.587
W2	1.664	2.211	1.911/1.909	1.899/1.897
W3	3.034	4.126	3.556/3.552	3.529/3.526
W4	4.328	5.919	5.004/4.999	4.965/4.960

TABLE 4.3. NATURAL FREQUENCIES OF 40 STOREY, 16 BAY PLANAR FRAME (rad/sec).

Results indicate that the frequencies obtained with the macroelement technique are well in between the upper and lower bounds provided by the TABS analyses. As in the static analysis of a planar frame, the macroelement technique provides a good approximation of the overall lateral stiffness.

Both the strain based and displacement based simple elements provide similar natural frequencies. The ratio of elastic properties of the equivalent membrane $\overline{E}_y / \overline{G}_{xy}$ is approximatively equal to 55 for this planar frame. With such a high ratio, it becomes apparent that the mode of deformation is predominantly one of shearing action. Under such conditions, the 6DOFS strain based element can only equal the results obtained with the displacement based 6DOFD element.

The refined elements produce natural frequencies that

are probably more accurate due to a higher number of degrees of freedom. The additional execution time however does not really justify their use since the simple elements required approximatively, only 57 % of the execution time used by the refined elements for only a very slight difference in results.

Other meshes were tested on this problem and all four elements were found to produce similar natural frequencies. The results however, are not realistic due to the improper mass distribution used in the coarser meshes.

4.4- ANALYSIS OF A CORE-SUPPORTED STRUCTURE

The strain based elements are now tested on the analysis of a concrete core-supported structure analysed by Stafford-Smith & Taranath [26]. The dimensions and loading arrangements are shown in Fig. 4.10. This relatively thin-walled core with a high aspect ratio deforms primarily in a bending mode when subjected to lateral loading. Moselhi [21], analysed this structure with his simple displacement based 6DOFD element and therefore it should prove interesting to compare his results to those obtained with the new strain based bending elements.

Due to the access openings, the core is unsymmetric producing warping stresses that equal the bending stresses [26]. A 3-dimensional analysis is thus required.

1.25 K/ft (18.24 KN/m)

12.5

15

187.5'

5' 10' 5'
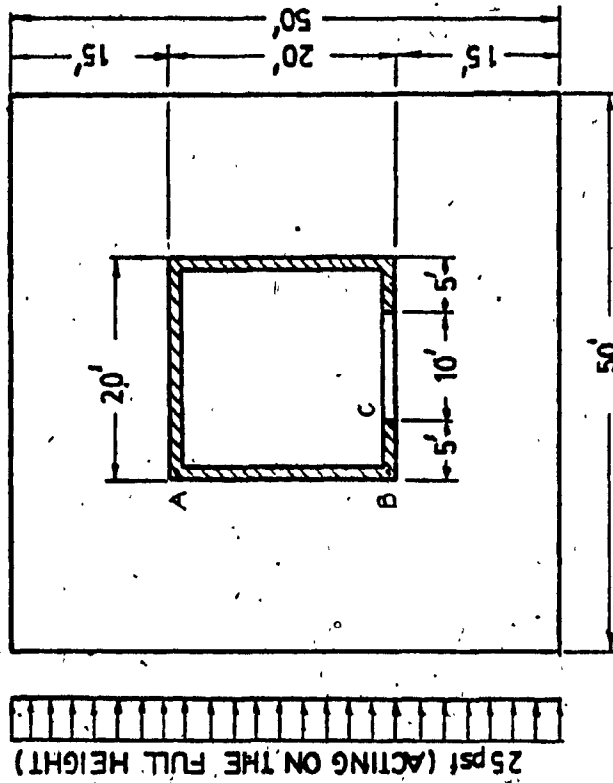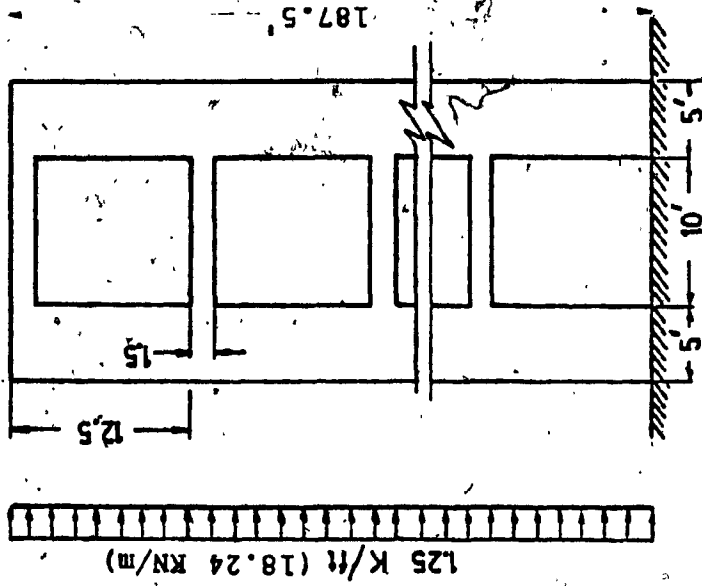
(b) ELEVATION OF SUPPORTING CORE

1' = .3048 m
1 psf = .04788 kPa

FIG. 4.10 - CORE-SUPPORTED STRUCTURE, [21]

15' 20' 15'

50'

50'

20'

5' 10' 5'

A

B

C

25 psf (ACTING ON THE FULL HEIGHT)

(a) PLAN

3x1.5'

10' 4.5'

FACADE #1

12.5'

7x25'

5x3.8'=19'

OTHER FACADES
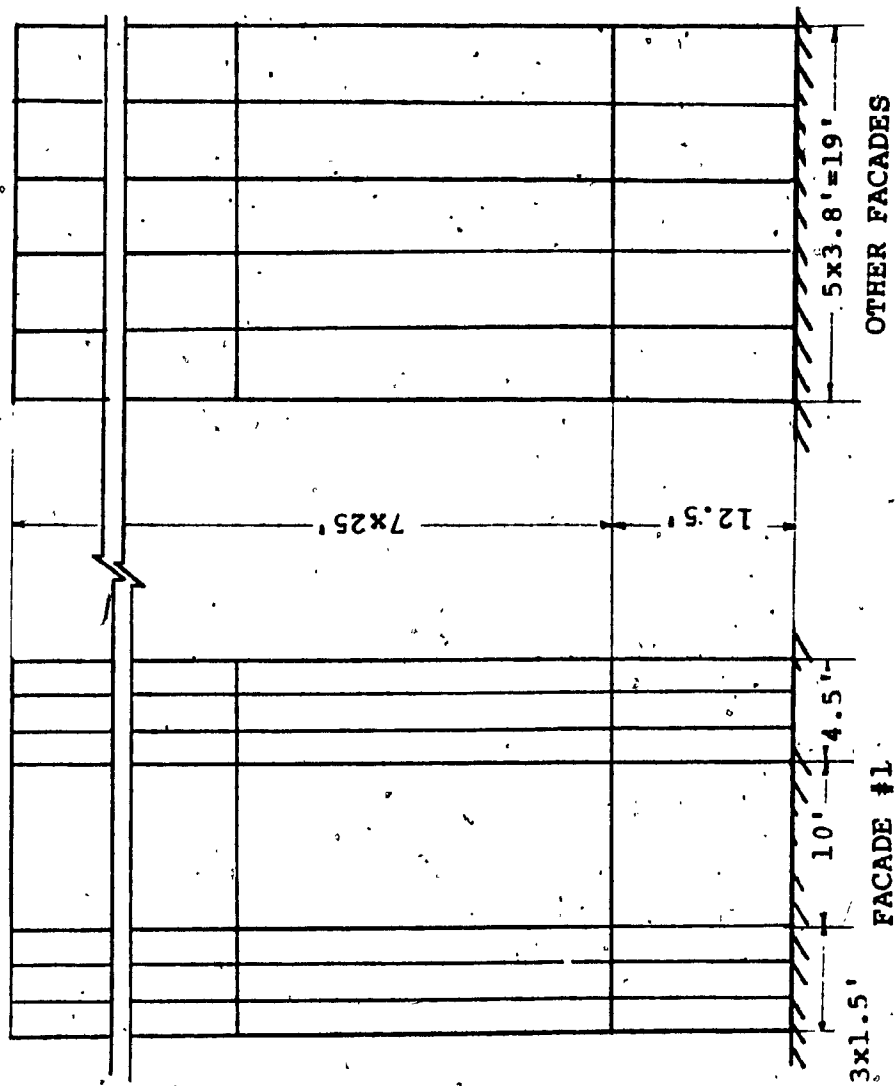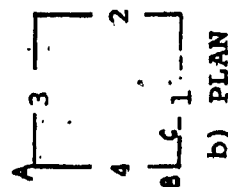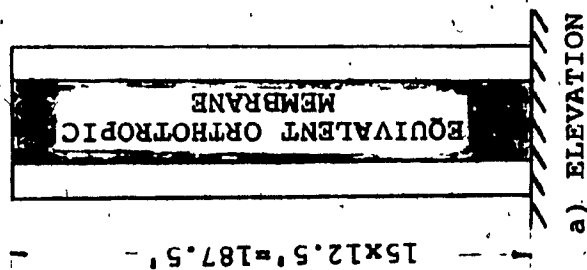
c) STRUCTURE IDEALIZATION

(1' = 0.3048 M)

EQUIVALENT ORTHOTROPIC
MEMBRANE

15x12.5'=187.5'

a) ELEVATION

A
3
4
2
B
1

b) PLAN

FIG. 4.11 - MODELLING OF CORE-SUPPORTED STRUCTURE

With the macroelement technique, the band of lintel beams is first replaced by an elastically equivalent orthotropic membrane with a uniform thickness of one foot. The equivalent closed tube is then discretized into a 3-dimensional assembly of finite elements as shown in Fig. 4.11. The mesh consists of 176 elements: 8 along the

| METHOD OF ANALYSIS | MAX.ROT. X.001 RAD | STRESS (ksf) AT | | |
		A	B	C
MACLEOD & HOSNY [20]	2.8	83.09	12.96	-90.43
STAFFORD-SMITH & TARANATH [26]	2.95	92.59	8.35	-75.31
KHAN & STAFFORD-SMITH [18]	3.32	91.73	8.78	-73.87
6DOFD	2.85	81.02	14.09	-72.42
6DOFS	3.38	86.07	15.68	-71.94
9DOFD	3.37	85.54	15.47	-71.74
8DOFS	3.38	86.36	15.74	-72.11

TABLE 4.4. COMPARAISON OF RESULTS FOR CORE-SUPPORTED STRUCTURE.

height and 22 elements around the perimeter.

The variation of floor rotations with height and the stresses at the base of the core structure using both simple and refined elements are obtained and compared to those of: (1) Stafford-Smith & Taranath [26]; (2) Khan & Stafford-Smith [18] and (3) Macleod & Hosny [20]. The results are presented in Table 4.4.

Macleod & Hosny used a discrete modified frame method and the authors of (1) and (2) employed Vlasov's theory for thin-walled elastic beams on an open and closed section respectively. The closed section analysis of Khan & Stafford-Smith [18] can be considered closer to the exact solution because they alone account for the shift of the shear center from its location in an open section (caused by the band of lintel beams). By analysing a closed section the circulatory St-Venant shear stresses across the coupling beams are taken into account.

The analysis of an open section does not really represent the true behaviour of the core assembly. The effective shift of the shear center towards the centroid of the section caused by the presence of the lintel beams is neglected. If the coupling beams are stiff then shear flow can travel along the contour and this cannot be neglected. A closed section analysis therefore offers a more rational assessment of the behaviour of the core assembly.

Examination of the maximum rotation as obtained by the various methods in Table 4.4 indicates that the 6DOFD element is indeed too stiff for a prevailingly bending deformation mode. The simple strain based 6DOFS element on the other hand hand produces similar results as those obtained with the higher order refined elements.

The efficiency of the simple strain based element is demonstrated by comparing the total number of degrees of freedom used in modelling the core structure. 240 DOF were
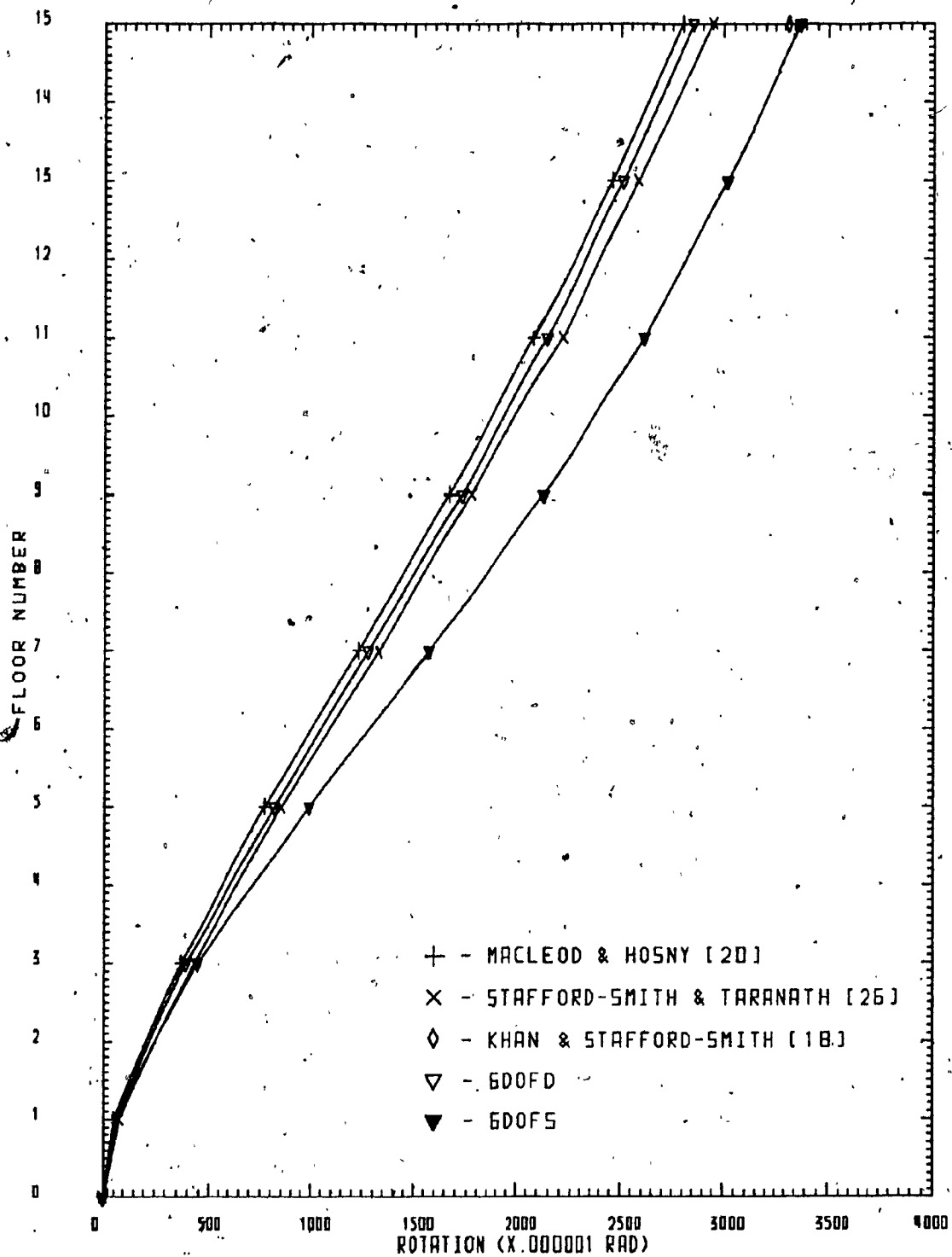
FIG. 4.12 – VARIATION OF FLOOR ROTATIONS WITH HEIGHT IN
CORE-SUPPORTED STRUCTURE

used with both simple elements, 448 DOF with the 9DOFD element and 416 DOF with the 8DOFS element. Thus, approximatively 45 % reduction in DOF (and a similar decrease in computation time using the TUBE program) with comparable results.

The floor rotations along the core height obtained by using the simple elements and those obtained by the other methods are shown in Fig. 4.12. Although the 6DOFD element agrees with the results from the open section analyses of Macleod & Hosny [20] and Stafford-Smith & Taranath [26], the 6DOFS element compares well to the maximum rotation obtained by Khan & Stafford-Smith [18] using the more appropriate closed section analysis.

The simple strain based element has now be shown to be a good element for the analysis of a corewall assembly. With such an element the macroelement technique can now be applied to the case of framed tube structures with service cores, i.e., "tube in tube" structures. With the continuum analogy, the problem of combining shear/corewalls to planar frames or framed tubes is easily accomplished. No other method of analysis can handle such a "composite" structure.

4.5- DYNAMIC ANALYSIS OF A BOX CANTILEVER BEAM

A box cantilever beam is now analysed for natural frequencies. The properties and dimensions of the structure

Z

48"

X

ground motion

(b) Elevation

level No.

4 × 12"

2 × 3"

Facade No. 1

level No.

4

3

2

1

3"

Facade No. 2

(c) Structure Idealization (Mesh 1)

Y

6"

1"

X

12"
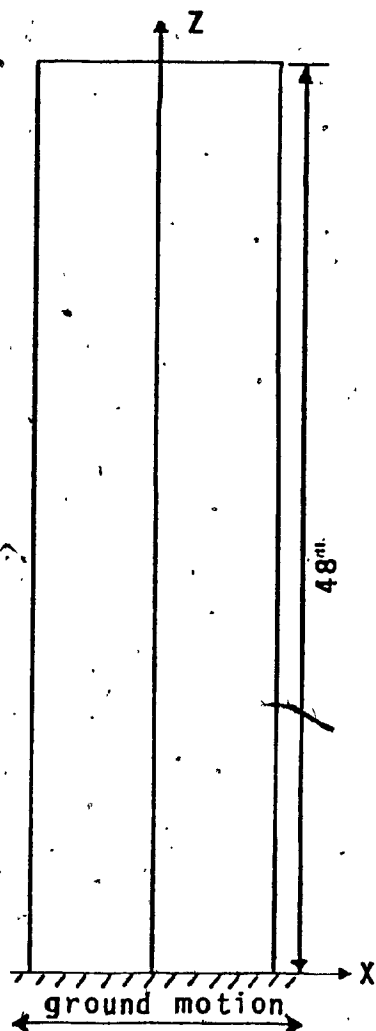
ground motion
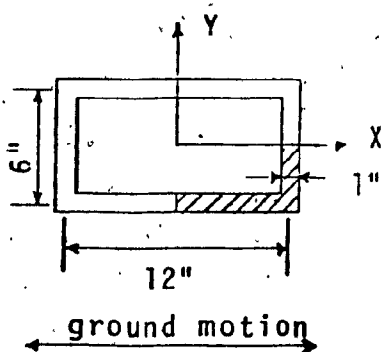
(a) Plan
Only the shaded portion
is modelled
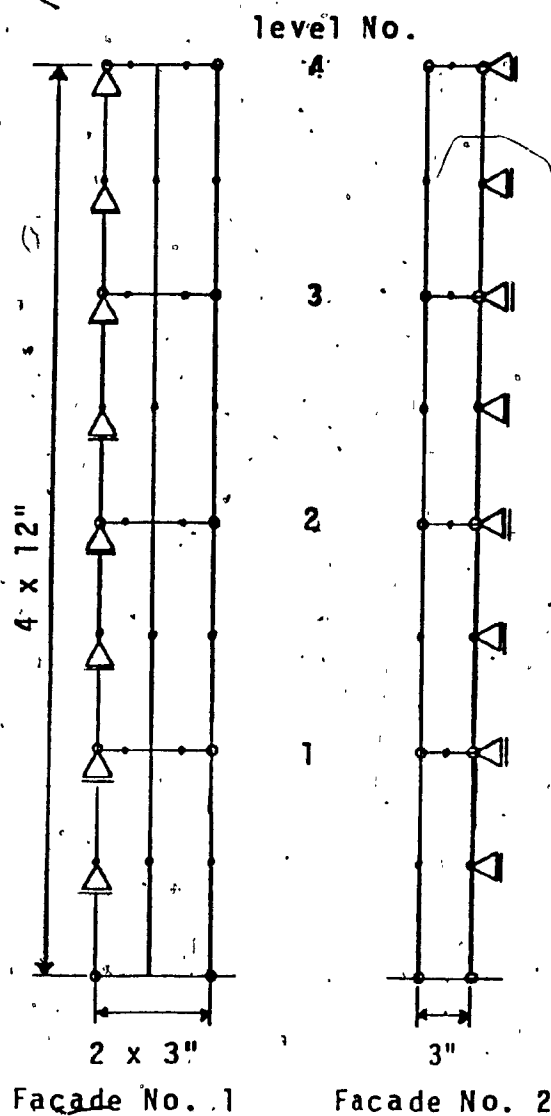
(d) Properties (steel)
Young's modulus 30000 ksi.
Poisson's ratio 0.25
specific weight 0.284 lb/in^3

1"=25.4 mm
1 ksi = 6894.8 kPa
1 lb/in^3 = .00927 Kg/m^3

FIG. 4.13 – BOX-CANTILEVER BEAM, [23]

are given in Fig. 4.13. This hollow steel shaft was analysed by Mule [23] with the refined 9DOFD element. The macroelement results will be compared to those obtained by engineering beam theory and to Goodno's and Gere's superelement method [11].

The 32-DOF box shaped superelement of Goodno and Gere is an assembly of a conforming plate bending element and a refined plane stress element. Eight such elements were used to model the rectangular shaft. An assembled lumped mass formulation was used to arrive at the mass matrix.

In the present method, the analysis commences directly with discretization of the 3-dimensional continuum. A mesh consisting of 12 elements (Fig. 4.13), is used and the mass is consequently lumped on 4 levels. The results from engineering beam theory which include shear deformations are considered here to be exact. Table 4.5 gives the first four frequencies of the shaft as obtained by the various methods.

The efficiency of the present method is demonstrated by comparing it to the superelement method. Both the macroelement method, using the 6DOFS or refined 9DOFD and 8DOFS elements and the superelement method give comparable results. The 6DOFD element is clearly too stiff in this predominantly bending deformation mode. The simple strain based 6DOFS element and the refined displacement based 9DOFD element require only 1/22 and 1/11 th of the total number of degrees of freedom used with the superelement respectively,

	Beam Theory	Super-Element	TUBE	
			SIMPLE 6DOFD/6DOFS	REFINED 9DOFD/8DOFS
Num of elements	---	8	12	12
Total DOF	inf.	352	16	32/28
Struct. DOF	inf.	16	4	4
W1	1186	1267	1357/1272	1271/1270
W2	5815	5702	6015/5781	5776/5756
W3	13189	12992	12039/11718	11751/11667
W4	21488	21162	16107/15865	15974/15829

TABLE 4.5. FIRST FOUR NATURAL FREQUENCIES OF BOX
        CANTILEVER BEAM (rad/sec).

and only 1/4 of the global (retained) degrees of freedom.

In this example, the simple 6DOFS element and the refined elements produce similar results. The simple strain based element on the other hand requires only half as many degrees of freedom. The new strain based element has once again proven to be an efficient simple element.

4.6- THE STRAIN BASED ELEMENTS AND THE MACROELEMENT
     TECHNIQUE

In Chapter III, the 6DOFS element was shown to be far superior to the 6DOFD element in simulating bending

- 94 -

behaviour. The results indicated that the simple strain based element converged more rapidly to exact results. However, when applied to the analysis of tall frame structures, the superiority of the 6DOFS element over the 6DOFD element was not as pronounced.

The reason for this is that the ratio of bending to shear deformations (DELTA-B/DELTA-S) of a solid section is far greater than that of a perforated section. The ratio of bending to shear deformations of a cantilever beam of rectangular cross section may be written as:

$$\text{DELTA-B/DELTA-S} = C \ (AR)^2 \ G_{xy}/E_y \qquad (4.1)$$

where the constant C is a function of the type of loading, AR is the aspect ratio of the beam and G_{xy} and E_y are the elastic modulii of the material. In spite of the fact that the amount of bending varies with the square of the aspect ratio, it also is a function of the stiffness parameters $\overline{G}_{xy}$ and $\overline{E}_y$ of the equivalent membrane. For isotropic materials, the ratio G_{xy}/E_y is equal to $1/2(1+\nu) = .35$ to .45, ($\nu = .45$ to .10)

In the case of an elastic orthotropic membrane simulating a perforated wall, the ratio of bending to shear deformations is generally much lower. The $\overline{G}_{xy}/\overline{E}_y$ ratio of a typical equivalent membrane usually ranges from .015 to .15. For example in the planar frame of Sec. 4.2, this ratio worked out to be .041. The aspect ratio of the 40 storey frame was equal to 5 and the constant C, for a

uniformly distributed loading, equal to 2.0. Placing these values into Eq. (4.1) indicates that bending accounted for only 67 % of the maximum lateral deflection. The simple strain based element is found to be only more efficient than the simple displacement based element when bending deformations account for 90 % or more of the maximum lateral deflection. This is shown in Fig. 4.14 which indicates the effectiveness of the simple elements as the ratio of bending to shear deformations is increased.

This graph was obtained by analysing a cantilever beam of rectangular cross section subjected to a uniformly distributed load. Various bending to shear deformation ratios were obtained by varying the aspect ratio and making use of Eq. (4.1). Results were then compared to those obtained by engineering beam theory. A 2x10 mesh of elements was used in the analysis as shown in Fig. 4.14. Points for DELTA-B/DELTA-S fewer than 10 could not be obtained as this results in a beam with an aspect ratio less than 4 and results from beam theory can no longer be considered as valid.

In conclusion to this point the 6DOFS element can only be expected to improve the results obtained by the 6DOFD element if the ratio G_{xy}/Ey is greater. This was demonstrated in the examples of Sections 4.4 and 4.5 in the analysis of solid sections. In these examples the 6DOFD element was found to be too stiff while the 6DOFS element produced results equal to those of the higher order refined
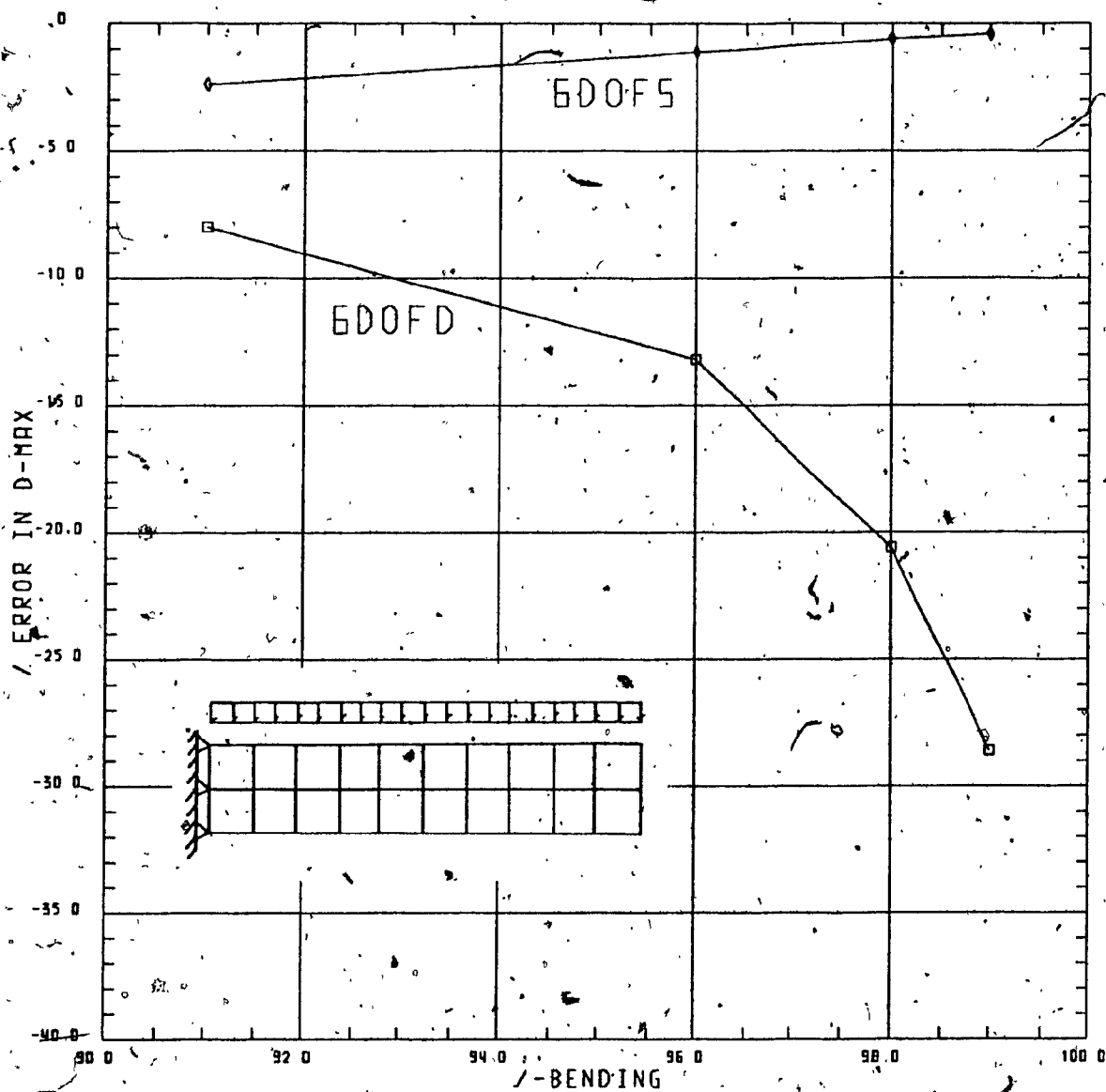
FIG. 4.14 - BENDING AND THE SIMPLE ELEMENTS

elements. Note that in framed tubes with a small amount of shear lag, i.e: with good tube action, a higher $\bar{G}_{xy} / E_y$ ratio is achieved by deeper spandrel beams.

A possible disadvantage to the 6DOFS as a macroelement is its low order, or simple state. A macroelement, which may span other several bays and storeys should be able to properly express the stress variation across its span. Low order elements, depending on the mesh, may not be able to express this variation adequately.

The refined strain based 8DOFS element, on the other hand, is well suited for this problem. It was found that by using a strain approach, a DOF could be removed from the 9DOFD element without any significant loss in accuracy. But as was pointed out earlier, an adequate method for determining the internal member forces from the stresses in the continuum has not yet been found.

In conclusion, the overall parameters such as maximum lateral deflection and natural frequency are not significantly affected by. the choice between the simple strain based element and the refined elements. The 6DOFS element is therefore recommended for genereal use in this macroelement technique. This simple element is specially well suited for the analysis of shear/corewalls where bending is predominant.

Keeping in mind that the macroelement technique is an approximate analysis method, the simple 6DOFS element can provide a designer with an acceptable approximation without

the need of going to a higher order element.

CHAPTER V

LIMITATIONS OF THE
MACROELEMENT TECHNIQUE

5.1- INTRODUCTION

The search for finite elements for use in macroelement analysis requires a good understanding of the technique. The salient qualities and deficiencies of the macroelement technique found throughout this study are presented in this chapter.

5.2- QUALITIES OF THE MACROELEMENT TECHNIQUE

Generally speaking, the macroelement technique is an efficient, simple to use, approximate method of analysis of framed tube structures. The method applies to multi-storey, multi-bay frames having a wide range of aspect ratios and stiffnesses, coupled shear walls, clad frames, planar and tubular structures consisting of frame and shear wall assemblies, and core-supported structures.

The numerical examples of macroelement analysis of the last chapter demonstrated that the technique is good for evaluating overall behavioural parameters such as structure displacements or natural frequencies. The method is

therefore highly recommended for this purpose because of the relatively small amount of computational effort.

5.3- DEFICIENCIES IN THE MACROELEMENT TECHNIQUE

The inability of the macroelement technique to provide reasonable results for the analysis of tall frame structures with Moselhi's simple element without increasing computational effort was the first defect. This was caused by the poor performance of his simple element when subjected to a predominant bending deformation mode. This defect was the focus of the present study and has been corrected with the new simple strain based element. There is however, further room for improvement in the macroelement technique.

5.3.1- BOUNDARY EFFECTS

The concept of deriving the elastic properties of the equivalent membrane from the deformation modes of a beam-column grid unit bounded by four inflection points is a big source of approximation. It would be fairly simple to examine the effect of using a more appropriate half grid unit to produce a special set of equivalent elastic properties along the edges or boundaries of the membrane.

As the number of bays and stories increases in a frame,

the error caused becomes negligable and the complete grid approximation becomes more acceptable. A limitation for the technique for a more precise number of bays and stories would be worth investigating.

However, the equivalent elastic properties as they are, have been shown to be quite accurate for the evaluation of the overall system parameters mentionned previously. The additional burden of requiring a special mesh of elements for this new set of equivalent elastic properties may render the technique less efficient without increasing the accuracy.

5.3.2- LOCATION OF INFLECTION POINTS

Tall slender structures subjected to lateral loading cause points of contraflexure to deviate from mid-span in the lower stories and outer bays. When this happens, the internal member forces obtained by the macroelement technique at these locations are severely upperbound. For example, in the 40 storey 14 bay planar frame of Sec. 4.2, the inflection point in the corner column of the first floor (of height H), is situated at 0.6 H from the bottom. The axial force in the column as obtained by the macroelement technique is approximatively 31 % higher than the axial force obtained from the (upperbound) TABS CL analysis. This amount of error can no longer be considered acceptable.

Generally as the number of bays is increased, the inflection points tend to locate themselves at mid-span. The error induced by the assumption of inflection points at mid-span is also more pronounced in the edge columns than in the innermost columns. Furthermore, the inflection points in the lower stories deviate from mid-span as the number of stories is increased.

5.3.3- INTERNAL MEMBER FORCES

The present method for determining the internal member forces is inadequate. Theoretically, it produces zero shear force in the outer columns and it severely overestimates the column axial forces in the lower floors for a tall slender structure. A new scheme for determining these internal member forces is therefore required.

In order to be efficient, it is believed that such a new scheme for internal member force evaluation should account for:

- special treatment for the members located along the edges of the frame.

- special treatment of the problem caused by the members whose inflection points are not located at mid-span, such as the members in the lower floors.

- Should account for the particular stress variation of the element being used (6DOFS or 8DOFS).

The last point is an important one. The true variation of internal member forces within a frame is more complex than the variation offered by the existing macroelements. A macroelement may span several bays and stories and therefore should be able to approximate this variation in an adequate manner. The understanding of the interpolating capabilities of a macroelement is also essential for proper mesh selection.

CHAPTER VI

CONCLUSIONS

Two strain based finite elements (simple and refined) have been developed for tall building analysis. After extensive testing these new elements were shown to be superior to similar displacement based elements. This superiority manifests itself either by improved performance or by the use of fewer degrees of freedom.

Parasitic shear in the existing simple displacement based, linear element makes a structure too stiff when subjected to a predominantly bending deformation mode. The new strain based 6DOFS element performs remarkably well in both shear and bending deformation modes and its fast convergence rate make it a better suited element for macroelement analysis.

Both refined elements, the strain based 8DOFS and the displacement based 9DOFD, perform well in all cases. The effectiveness of these elements is attributed to their higher order. It has been shown that with a strain based approach, the 8DOFS element is equally effective or better than the 9DOFD element in both convergence rate and accuracy.

When the 6DOFS element is applied to the macroelement technique of analysis of a perforated wall of a framed tube, the improvement in results is only marginal. This is

because of the predominantly shear racking mode of deformation in the frame. The 6DOFS element does however, provide good approximate results.

In the analysis of shear walls, coupled shear walls, corewalls or any solid sections where bending is predominant, the simple strain based 6DOFS element is a very efficient element.

For general use, it is therefore recommended that the 6DOFS strain based element be adopted. Any supposedly increase in accuracy achieved by the refined elements does not seem to warrant their use because of the significant increase in computer time.

The refined strain based 8DOFS element with its better interpolating capabilities however, may prove to be useful with a new scheme for determining internal member forces.

REFERENCES

[1]   Ast, P.F., and Schwaighofer, J., "Economical Analysis of Large Framed-Tube Structures", Building Science, Vol.9, 1974, pp.73-77.

[2]   Chan, P.C.K., "Static and Dynamic Analysis of Framed-Tube Structures", Ph.D.Thesis, McMaster University, Hamilton, Canada, 1973.

[3]   Cheung, Y.K., and Swaddiwudhipong, S., "Analysis of Frame Shear Wall Structures Using Finite Strip Elements", Proc.Instn.Civ.Engrs., Part 2, 1978, 65, Sept., pp.517-535.

[4]   Cook, R.D., Concepts and Applications of Finite Element Analysis. 2d Ed., John Wiley & Sons Inc., New York, 1981.

[5]   Coull, A., and Bose, B., "Simplified Analysis of Framed-Tube Structures", J.Struct.Div., ASCE, Vol.101, No.ST11, Nov.1975, pp.2223-2240.

[6]   Coull, A., and Subedi, N.K., "Coupled Shear Walls with Two and Three Bands of Openings", Building Science, Vol.7, 1972, pp.81-86.

[7]   Coull, A., and Subedi, N.K., "Framed-Tube Structures for High-Rise Buildings", J.Struct.Div., ASCE, Vol.97, ST8, Aug.1971, pp.2097-2105.

[8]   Council on Tall Buildings, Group CB, 1978, Structural Design of Tall Reinforced Concrete and Masonry Buildings, Vol.CB of Monograph on Planning and Design of Tall Buildings, ASCE, New York.

[9]   Council on Tall Buildings, Group SB, 1979, Structural Design of Tall Steel Buildings, Vol.SB of Monograph on Planning and Design of Tall Buildings, ASCE, New York.

[10] DeClercq, H., "Analysis and Design of Tube-Type
      Tall Building Structures", Ph.D.Thesis, University
      of California, Berkeley, 1975.

[11] Goodno, B.J., and Gere, J.M., "Analysis of
      Shear Cores Using Superelements", J.Struct.Div.,
      ASCE, Vol.102, No.ST1, Jan.1976, pp.367-383.

[12] Ha, K.H., Fazio, P., and Moselhi, O., "Orthotropic
      Membrane for Tall Building Analysis",
      J.Struct.Div., ASCE, Vol.104, No.ST9, Sept.1978,
      pp.1495-1505.

[13] Heidebrecht, C., and Stafford-Smith, B.,
      "Approximate Analysis of Open-Section Shear Walls
      Subjected to Torsional Loading", J.Struct.Div.,
      ASCE, Vol.99, No.ST12, Dec.1973, pp.2355-2373.

[14] Iyengar, S.H., "Stability of Overall Structural
      Systems", Proc. Int. Confer. on Planning and
      Design of Tall Buildings, Lehigh, Techn.Comm.No.16,
      Discussion No.4, Vol.II, 1972, pp.564-567.

[15] Khan, A.H., "Analysis of Tall Shear Wall-Frame and
      Tube Structures", Ph.D.Thesis, University of
      Southampton, U.K., March 1974.

[16] Khan, F.R., and Amin, N.R., "Analysis and Design
      of Framed Tube Structures for Tall Concrete
      Buildings", The Structural Engineer, No.3, Vol.51,
      1973, pp.85-92.

[17] Khan, A.H., and Stafford-Smith, B., "A Simple
      Method of Analysis for Deflection and Stresses in
      Wall-Frame Structures", Building and Environment,
      Vol.11, 1976, pp.69-78.

[18] Khan, M.A.H., and Stafford-Smith, B., "Restraining
      Action of Bracing in Thin-Walled Open Section
      Beams", Proc.Instn.Civ.Engrs., Part 2, 1975, 59,
      March, pp.67-78.

[19] Liauw, T.C., "Evolution of New Structural Systems for Tall Buildings", Proc. Regional Confer. on Tall Buildings, Bangkok, ASCE-IABSE Joint Committee, Jan.1974, pp.115-125.

[20] Macleod, I.A., and Hosny, H.M., "Frame Analysis of Shear Wall Cores", J.Struct.Div., ASCE, Vol.103, No.ST10, Oct.1977, pp.2037-2047.

[21] Moselhi, O., "Analysis of Perforated Walls and Tube-Type Tall Building Structures", Ph.D.Thesis, Concordia University, Montreal, 1978.

[22] Moselhi, O., Fazio, P., and Zielinski, Z., "Simplified Analysis of Wall-Frame Structures", J.Can.Soc. of Civ.Engrs., Vol.5, No.2, June 1978, pp.262-273.

[23] Mule, A., "Dynamic Analysis of Tall Planar and Tube-Type Building Structures", M.ENG.Thesis, Concordia University, Montreal, 1983.

[24] Sabir, A.B., "Private Communications with Ha, H.K.".

[25] Santhakumar, A.R., "Analysis of Non-Uniform Coupled Shear Walls with Two Rows of Openings", Proc. Intern. Symposium on Earthquake Structural Engineering, St-Louis, Aug.1976, pp.1249-1262.

[26] Stafford-Smith, B., and Taranath, B.S., "The Analysis of Tall Core-Supported Structures Subjected to Torsion", Proc Inst. of Civ.Engrs., Vol.53, Sept.1972, pp.173-187.

[27] Wilson, E.L., and Dovey, D.H., "Three Dimensional Analysis of Building Systems-TABS", University of California, Berkeley, 1972.